

Distribution Agreement

In presenting this thesis as a partial fulfillment of the requirements for a degree from Emory University, I hereby grant to Emory University and its agents the non-exclusive license to archive, make accessible, and display my thesis in whole or in part in all forms of media, now or hereafter now, including display on the World Wide Web. I understand that I may select some access restrictions as part of the online submission of this thesis. I retain all ownership rights to the copyright of the thesis. I also retain the right to use in future works (such as articles or books) all or part of this thesis.

Camila Sofia Makhlouta Lugo

March 30th, 2020

Morphological Characterization of Thoracic Paravertebral Post-Ganglionic Neurons during
Development in the Mouse

by

Camila Sofia Makhlouta Lugo

Shawn Hochman, Ph.D
Adviser

Neuroscience and Behavioral Biology

Shawn Hochman, Ph.D
Adviser

Alan Sokoloff, Ph.D
Committee Member

Michael Crutcher, Ph.D
Committee Member

2020

Morphological Characterization of Thoracic Paravertebral Post-Ganglionic Neurons during
Development in the Mouse

By

Camila Sofia Makhlouta Lugo

Shawn Hochman, Ph.D

Adviser

An abstract of
a thesis submitted to the Faculty of Emory College of Arts and Sciences
of Emory University in partial fulfillment
of the requirements of the degree of
Bachelor of Science with Honors

Neuroscience and Behavioral Biology

2020

Abstract

Morphological Characterization of Thoracic Paravertebral Post-Ganglionic Neurons during Development in the Mouse

By Camila Sofia Makhlouta Lugo

The sympathetic nervous system represents one major system involved in the autonomic control of body function. The entire central sympathetic output arises from spinal cord pre-ganglionic neurons located in thoracic and upper lumbar spinal segments that project to sympathetic post-ganglionic neurons (SPNs). SPNs innervate target organ systems. Most are embedded in paravertebral sympathetic chain ganglia that provide broad distributed control of cardiovascular and thermoregulatory systems. Very little is known about the morphology and plasticity of SPNs in thoracic chain ganglia across post-natal development. Furthermore, few studies have been conducted in mice. This thesis undertook detailed morphological characterization of individually-reconstructed SPNs in the mouse fifth thoracic ganglia at three key developmental time points; weaning (PND 21), adolescence (PND 35) and adulthood (PND 60+). To visualize individual SPNs for unbiased morphological reconstruction, I used sparse labeling tyrosine hydroxylase (TH)-Cre :: tdTomato-reporter mice that resulted in stochastic recombination-based labeling in ~6% of SPNs. I compared developmental changes in cell soma volume and several dendritic properties. Surprisingly, no age-dependent changes in cell volume was seen, though there was significant inter-age variability (at PND 21 and 60+). PND 21 SPNs had the highest number of primary dendrites. SPNs possessed branching and un-branching dendrites. PND 35 SPNs had the highest and PND 60+ had the lowest fraction of branching dendrites. Primary dendrite length of branching dendrites was shortest at PND 21 while PND 60+ SPNs had the longest un-branching dendrites. Overall results support a prominent age-dependent lengthening of dendrites. An unanticipated observation was the immense variation in morphology seen between mice of the same age. This may reflect differences in subpopulation of SPNs sampled by stochastic sparse labeling. Additionally, as considerable SPN connectivity occurs post-natally, variation in early-life experience may also contribute to inter-animal variability. In summary, unbiased labeling identified SPNs as possessing a broad range of morphological variability but with classifiable differences in dendritic properties during post-natal developmental. By using mice as the *de facto* genetic mammalian model, this work helps lay the foundation for future studies on SPN organization and plasticity including in disease models of autonomic dysfunction.

Morphological Characterization of Thoracic Paravertebral Post-Ganglionic Neurons during
Development in the Mouse

By

Camila Sofia Makhoulouta Lugo

Shawn Hochman, Ph.D

Adviser

A thesis submitted to the Faculty of Emory College of Arts and Sciences
of Emory University in partial fulfillment
of the requirements of the degree of
Bachelor of Science with Honors

Neuroscience and Behavioral Biology

2020

Acknowledgements

To my PI and advisor, Dr. Shawn Hochman: thank you for your constant support, attention and passion in introducing me to the field of neuroscience research and welcoming me into your lab. I am incredibly grateful for all the time, resources and efforts that you and your team have invested in me and hope that future neuroscience students can be first exposed to research in such a supportive, friendly yet ambitious environment.

To my advisor and thesis committee member, Dr. Alan Sokoloff: thank you for being so attentive, caring, informative and supportive of my collegiate research journey. All the time you have invested in my education and training has truly changed how I view the field of research and has elevated my education at Emory in ways that I could have never imagined. You have been an immense mentor to me throughout my college career and I hope to take all the advice you have given me throughout the years into my future as a scientist.

To Michael Sawchuk: thank you for all the time and effort you invested into my project, answering my questions and training me in research methodologies. Your incredibly skilled work in dissections and the entirety of the immunohistochemistry of this project has made this thesis possible and for that I am very thankful.

To Dr. Francisco Alvarez: thank you for allowing us to use your Confocal microscope and welcoming us into your lab. Without your generosity, this project would not have been possible.

To my thesis committee and advisor, Dr. Michael Crutcher: thank you for all the guidance you have given me since the moment I declared the Neuroscience and Behavioral Biology major. Your advice has been pivotal in my college career and all the lessons, in class and out, have fundamentally shaped my future goals.

To Dr. Roesch: thank you for all your encouragement and support throughout this process. Your words of motivation and your moral support undoubtedly helped me push through the final stages of this thesis. Thank you for constantly advocating for your students and always having our best interests in mind. I am grateful for all the time you dedicated to listening and hearing my concerns, acknowledging my struggles and helping me objectively overcome them.

To Makalele Provost: thank you for being a mentor to me as I first joined the lab. Answering all my questions, involving me in projects and motivating me to continue on the path of research all the while conducting your own dissertation and managing all your responsibilities.

To everyone in Dr. Hochman's lab: thank you for being such a supportive, encouraging and caring team that made me excited about research and going into lab every week. I am eternally grateful for the wonderful environment I was in during a time of immense growth.

Table of Contents

1.	Introduction and Background	1
1.1	<i>Overview</i>	1
1.2	<i>The Sympathetic Nervous System</i>	2
1.3	<i>Functional Implications of Morphological Measures</i>	5
1.4	<i>Development of Sympathetic Chain Ganglia Neurons</i>	6
1.5	<i>Hypothesis</i>	10
2.	Materials and methods	10
2.1	<i>Subjects</i>	10
2.2	<i>Age Categories: Developmental Aspect</i>	14
2.3	<i>Tissue Preparation, Imaging and Tracing</i>	14
2.4	<i>Data Analysis</i>	18
3.	Results	19
3.1	<i>Neuron Number Across Development</i>	19
3.2	<i>Primary Dendrite Number Across Development</i>	20
3.3	<i>Comparing Incidence of Primary Dendrite Branching Across Development</i>	22
3.4	<i>Comparing Dendrite Length Across Development</i>	24
3.4	<i>Cell Body Volume Across Development</i>	28
3.5	<i>Rostro-caudal Analysis</i>	32
3.6	<i>TH+ and Td+ Cell counts</i>	34
4.	Conclusion	35
5.	Discussion	37
5.1	<i>Implications of Morphological Trends: Dendritic Arborization</i>	37
5.2	<i>Implications of Morphological Trends: Cell size</i>	40
5.3	<i>Individual and Rostro-caudal Variability</i>	41
5.5	<i>The Sparse Label</i>	43
5.6	<i>Body Size as a Confounding Variable</i>	46
6.	References	46

Figures

<u>Figure 1</u> : Sympathetic Nervous System General Neural Pathway	1
<u>Figure 2</u> : <i>Organization and Innervations of Sympathetic Neurons</i>	2
<u>Figure 3</u> : Gross Anatomy of the tSCG.	3
<u>Figure 4</u> : The monoamine synthesis pathways.....	11
<u>Figure 5</u> : The Cre-Lox System.....	13
<u>Figure 6</u> : Genetic cross in TH::Td Transgenic mice	13
<u>Figure 7</u> : Confocal Images and Reconstructions	16
<u>Figure 8</u> : Dendrogram of a Sympathetic neuron.....	18
<u>Figure 9</u> : Raw Td+ neuron counts in T5 ganglia at three developmental stages.....	20
<u>Figure 10</u> : Histogram of number of dendrites per neuron across development.....	22
<u>Figure 11</u> : Comparing incidence of branched and un-branched dendrites between ganglia in individual mice.....	23
<u>Figure 12</u> : (A-E) Histograms showing distribution of branched and un-branched primary dendrite length across development.....	26
<u>Figure 13</u> : (A-E): Cumulative sum graphs for branched and un-branched dendrite length	27
<u>Figure 14</u> : (A-B) Box and Whisker Plots for branched and un-branched primary dendrite length across development.....	28
<u>Figure 15</u> : Histogram of cell body volume across development.....	29
<u>Figure 16</u> : Cumulative sum graph of cell body volume across development.....	30
<u>Figure 17</u> : Box and Whisker plots for cell body volumes across development	31
<u>Figure 18</u> : Rostrocaudal differences in number of Td+ neurons	33
<u>Figure 19</u> : 4 consecutive thoracic ganglia of 3 adult mice	34
<u>Figure 20</u> : Tracings of the tSCG in adult mice	42
<u>Figure 21</u> : (A-E) T5 ganglia of PND69C.....	45

Tables

Table 1: Summary of Literature: Sympathetic Neurons Across Development.	9
Table 2: Primary antibodies used for immunocytochemistry.....	15
Table 3: Secondary antibodies used for immunohistochemistry	15
Table 4: Descriptive statistics of number of primary dendrites per neuron	21
Table 5: Descriptive statistics of branching data in neurons	23
Table 6: Difference between branching and un-branching dendrite length in individual mice T5 ganglia	24
Table 7: Descriptive statistics on branched vs. un-branched primary dendrite length.....	25
Table 8: Descriptive statistics on cell body volume across development.....	29
Table 9: Descriptive statistics of Contour data	32

1. Introduction and Background

1.1 Overview

The autonomic nervous system, a division of the peripheral nervous system, can be broken down into the sympathetic and the parasympathetic nervous systems. This research focuses on better understanding the anatomical organization of the sympathetic nervous system with specific focus on a group of post-ganglionic neurons in the paravertebral sympathetic chain

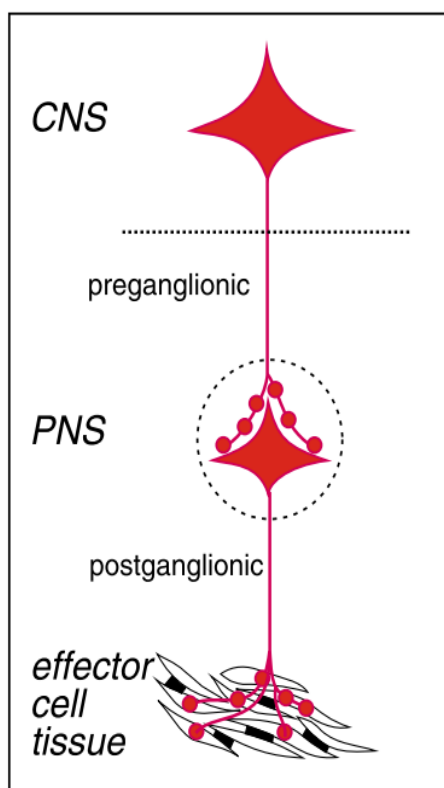


Figure 1: Sympathetic Nervous System General Neural Pathway
The organization of the sympathetic nervous system showing preganglionics synapses on postganglionics at the tSCG. Illustration adapted from (Jänig, 2014)

ganglia. Currently, relatively little is known about neuronal morphology and post-natal development of the thoracic sympathetic chain ganglia (**tSCG**). Moreover, the anatomical studies undertaken have not focused on the mouse even though the mouse is the predominant transgenic mammalian model system in neuroscience (Furlan et al., 2016). Given the importance of studies in mice as a model organism, I felt it crucial to characterize inter-animal and developmental differences in neuronal composition as the first but essential steppingstone to future studies on models of autonomic dysfunction seen clinically.

Below I provide a general introduction on the autonomic nervous system then focus the background on a review of our understanding of paravertebral sympathetic post-ganglionic neurons.

1.2 The Sympathetic Nervous System

Being part of the autonomic nervous system, the sympathetic nervous system is responsible for involuntary motor commands. Colloquially known as regulating our “fight or flight” response,

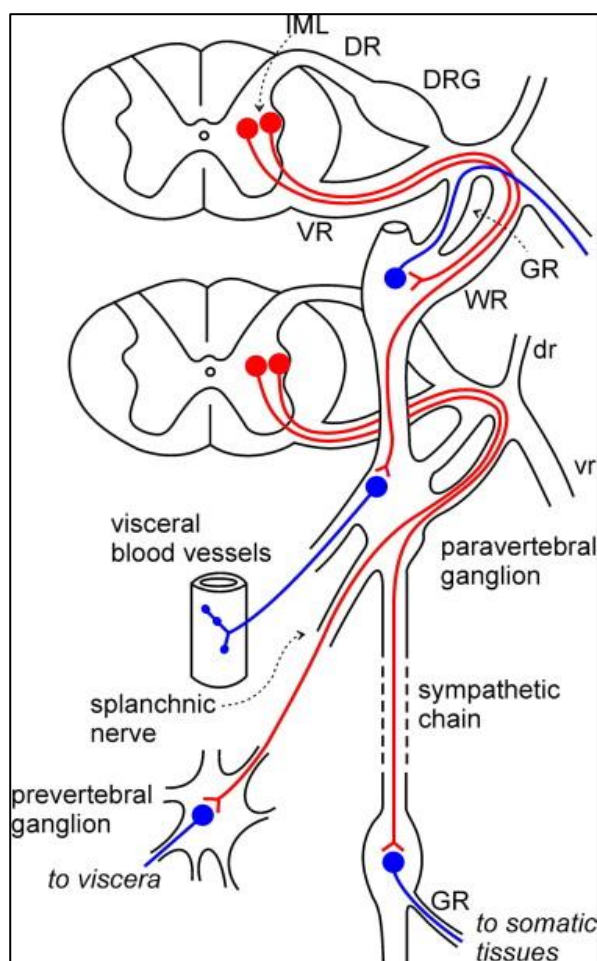


Figure 2: Organization and Innervations of Sympathetic Neurons

Depiction of the sympathetic nervous system innervations with preganglionic sympathetic neurons in red and SPNs in blue. Illustration from Jänig, W. (2006).

the sympathetic nervous system is also involved in maintaining homeostasis and coordinating thermoregulation. This response to stimuli involves whole-body processes and thus the neurons in this system innervate organ tissue throughout the entire mammalian body (Alshak and Das, 2020).

These neurons communicate to target tissue through a particular pattern of innervation and connectivity (as seen in *Figure 1*) which is notably similar to that of the parasympathetic nervous system (Jänig, 2014). The parasympathetic nervous system has a slightly different pattern of connectivity, having their ganglia near the target tissue. For the

sympathetic nervous system, two organizations of sympathetic ganglia are recognized, prevertebral ganglia located near to the organs of their innervation and paravertebral ganglia, located adjacent to the spinal cord in the posterior body wall. Sympathetic post-ganglionic neurons (**SPNs**) exit the ganglia and travel in peripheral nerves to reach their target organs (*Figure 2*). Examples of prevertebral ganglia are the celiac, superior mesenteric and inferior mesenteric ganglia (Szurszewski and Linden, 2012). Most of the sympathetic ganglia are in the paravertebral chain which can be visualized in *Figure 3*. The sympathetic ganglia are the contact point between

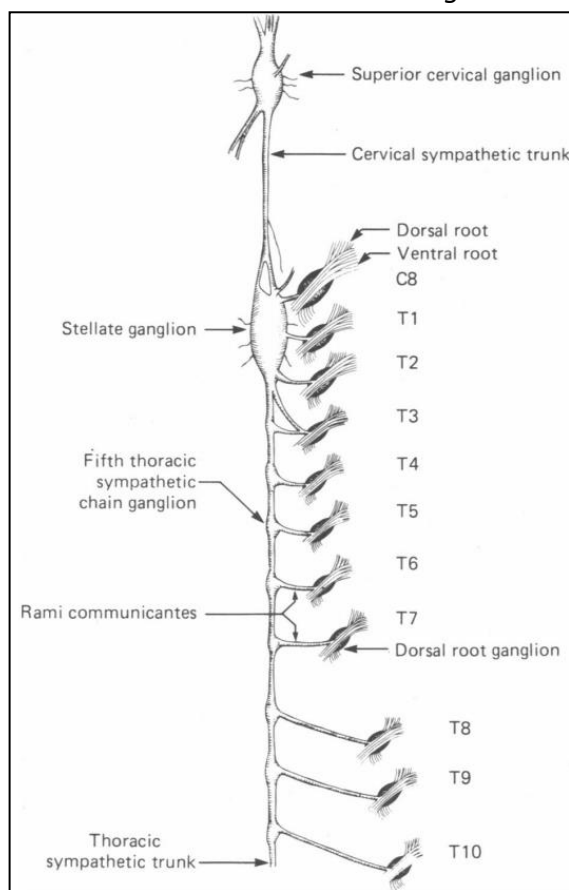


Figure 3: Gross Anatomy of the tSCG.

Closer depiction of the peripheral section of the sympathetic system, that is the tSCG. Illustrated by Lichtman and Purves in 1980, based off of anatomical studies in the guinea pig.

the preganglionic sympathetic neurons coming from the central nervous system and the SPNs innervating target organs. The preganglionic sympathetic neurons synapse on the SPNs using acetylcholine as their neurotransmitter while SPNs use noradrenaline as their neurotransmitter for communication with target organs. However, a small population of SPNs exist that are instead cholinergic. In the tSCG of the mouse these mainly synapse on eccrine sweat glands and skeletal muscle vasculature (Schafer et al., 1977) and constitute approximately 3-5% of the neuronal population (Masliukov and Timmermans, 2004; Choi, 2015).

Until recently the main function of the SPNs was thought to be limited to the relay of information from preganglionic sympathetic neurons to peripheral structures but recent publications suggest the SPNs have integrative capacity with some independence and flexibility with respect to information coming from the spinal cord (Kenney & Ganta, 2014). SPNs were thought to function as 1:1 relays for preganglionic sympathetic neurons, however in recent findings on preganglionic sympathetic neuron convergence onto SPNs, SPNs are more likely “continuously variable gates” with the capacity to interpret presynaptic activity (Bratton et al., 2010; Springer et al., 2015). In other words, summation from multiple preganglionic inputs may contribute to SPN activation raising the possibility that synaptic integration at the level of the SPN may contribute to the SPN regulation of target organ function (McKinnon et al., 2019). Studying the morphology of SPNs can increase our understanding of the mechanisms and origins of this regulation. Moreover, differences in post-ganglionic dendritic morphology in disease and injury may provide important insight into the emergent behavioral dysfunction seen. For example, the SPNs are implicated in a variety of pathologies as evidenced by the role they play in the formation of neuroblastomas (Chelmicka-Schorr et al., 1985) and their involvement in the pathophysiology of hypertension (Reid, 1992; Springer, 2015).

Developmentally, the sympathetic nervous system is actively maturing until around the second month of life in mammals (Masliukov, 2001). Furthermore, establishment of preganglionic inputs to post-ganglionic neurons and formation of primary dendrites has been documented to carry on long into post-natal development (Ernsberger, 2001; Snider, 1988). In fact, studies have shown the majority of dendritic growth occurs post-natally (Voyvodic, 1987a).

Furthermore, sympathetic neurons are unique in that they continue to divide after neuronal differentiation (Gonzalez et al., 2013; Rohrer and Thoenen 1987; Rothman et al., 1978). This suggests that the sympathetic nervous system is dynamically changing after birth, possibly to regulate, integrate or coordinate different biological needs during development. By analyzing morphology across development we can not only begin to understand the functional properties of these neurons but also the changes that occur post-natally as they relate to changing developmental needs.

1.3 Functional Implications of Morphological Measures

Structural analysis, such as the study of morphology, can provide insight into the various roles particular groups of neurons play in the nervous system. For example, cell body size has been seen to correlate with number of primary dendrites (Havton and Ohara, 1994). In 1985, Purves and Lichtman studied the morphology of neurons in the superior cervical ganglia (see *Figure 3*) with the hopes of better understanding their function (Purves & Lichtman, 1985). They found that convergence of preganglionic sympathetic neuron inputs to SPNs in the paravertebral ganglia was related to dendritic complexity and cell geometry amongst other things. A study investigating neuronal morphology of the tSCG was carried out with a focus on the chemical neuroanatomy of final sympathetic motor neurons (Gibbins et al., 2000). Gibbins et al. concluded that soma size is related to conduction velocity, that the dendritic tree can be used to predict preganglionic convergence onto SPNs and that neurons in different pathways could be distinguished based on morphology. Categorization of neurons based on morphology was seen to be accurate in additional studies. For example, Dodd and Horn (1993) showed that neuronal

functional subtypes could be distinguished by cell body diameter with >93% accuracy (Dodd and Horn, 1983). Lastly, in the cat and human stellate ganglion two neuronal subtypes were differentiable by morphology (Masliukov, 2001; Zshabotinsky, 1953). These studies demonstrate that morphology can provide important insight into the functional properties of SPNs.

1.4 Development of Sympathetic Chain Ganglia Neurons

Developmental studies can help us better understand functional roles neurons play as they relate to behavioral changes in maturity. Furthermore, characterizing the tSCG in mice across development is imperative before embarking on future studies. Developmental studies in rats and mice have shown that neurotransmitter composition is complete, that is, neuronal populations become similar to that of adults 60 days post-natally (Masliukov and Timmermans, 2004). Anatomical studies have also shown that development of sympathetic chain ganglia varies in a rostro-caudal fashion (Snider, 1986). Lichtman in 1979 found that pre-ganglionic sympathetic neurons seem to have an affinity for innervating SPNs on a rostro-caudal axis, that is, more rostral pre-ganglionic sympathetic neurons innervate more rostral SPNs (Lichtman, 1979). Furthermore, Jobling and Gibbins found morphological differences in SPNs in the rostral superior cervical ganglia versus the more caudal thoracic ganglia, (see *Figure 3*). Specifically, they found that thoracic SPNs had more extensive dendritic arbors which were rarely seen in the superior cervical ganglia. Furthermore >80% neurons of sympathetic chain gangli could be correctly attributed to their ganglion based on electrophysiological properties suggesting heterogeneity in morphology and function of sympathetic neurons (Jobling and Gibbins, 1999). This shift in rostro-caudal innervation and morphology suggests possible functional differences across the sympathetic

chain ganglia of the same animal. The functional relevance of this variation is not well understood and to further understand this a developmental model could be of use. If a rostro-caudal pattern or morphological trend is documented across development, this could help us understand functional differences as they relate to behavior.

Developmental analysis of the sympathetic chain ganglia has pointed to a few general morphological trends. Snider (1986) found that although there are rostro-caudal differences in the morphology of sympathetic chain neurons of neonates, this variation did not carry into maturity suggesting that patterns of dendritic growth and morphology change during development. Moreover, a previous study done on the superior cervical ganglia of rats suggests that dendrites continue to grow in adulthood (Voyvodic, 1987a). These two findings suggest a change in the pattern of growth and a systematic reorganization of the tSCG neurons during development.

Primary dendrite number and total dendritic length are a way of analyzing dendritic arborization that can speak volumes on the connectivity of a neuron. Andrew in 1993, studying the rat superior cervical ganglion from 6 weeks to 7 months post-natally, found the following trends in morphology across development: a decrease in primary dendrite number, increase in total dendritic length, an increase in soma size and an increase in the amount of dendritic branching (Andrews et al., 1993). This is in accordance with Voyvodic who found a 4-fold increase in dendritic length during the first post-natal month in rats.

With new technologies and research approaches we can uncover more about the morphology of such neurons and further understand their function. In this project I apply new

genetic tools to study morphology of SPNs in the adult mouse and explore how this morphology changes during development. Particularly, the genetic tool used here is the the Cre-lox system to create transgenic mice that exhibit a sparse subset of SPNs in tSCG. As noted previously, researchers have carried out studies analyzing the morphology of neurons in mainly the superior cervical ganglia across development, however very few studies have been carried out in mice and very few have examined thoracic ganglia due to their *in vivo* inaccessibility. Many powerful genetic tools are available in mice. Thus, characterizing the morphology of SPNs in the mouse during different post-natal stages will provide important information for subsequent studies in mouse.

Table 1: Summary of Literature: Sympathetic Neurons Across Development.

As can be noted, in general a decrease in neuronal density was seen across development. Morphological measures that increased across development were soma size and dendritic complexity measured through number of primary dendrites, dendritic length and dendritic branching. SCG; superior cervical ganglia.

	Mammal	Ganglia	Time period (PND)	[Increase/Decrease/No change] with age	Reference
Neuronal Density	Cat	Stellate	0-60	Decrease	<i>Masliukov, 2001</i>
Soma Size	Cat	Stellate	0-60	Increase	<i>Masliukov, 2002</i>
	Guinea Pigs	Celiac	Early fetal - Adult	Increase	<i>Anderson, Jobling and Gibbins, 2001</i>
	Rats	SCG	42-210	Increase	<i>Andrews, 1993</i>
Number of Primary Dendrites	Guinea Pigs	Celiac	Early fetal - Adult	Increase	<i>Anderson, Jobling and Gibbins, 2001</i>
	Rats	SCG	0-30	Increase	<i>Voyvodic, 1987</i>
	Rats	SCG	Post-natal period	No change	<i>Snider, 1988</i>
	Rats	SCG	42-210	Decrease	<i>Andrews, 1993</i>
Dendritic Length	Guinea Pigs	Celiac	Early fetal - Adult	Increase	<i>Anderson, Jobling and Gibbins, 2001</i>
	Rats	SCG	0-30	Increase	<i>Voyvodic, 1987</i>
	Rats	SCG	42-210	Increase	<i>Andrews, 1993</i>
Branching	Rats	SCG	210-720	Decrease	<i>Andrews, 1993</i>
	Rats	SCG	0-7	Increase	<i>Snider, 1988</i>
	Rats	SCG	0-30	Increase	<i>Voyvodic, 1987</i>

1.5 Hypothesis

My hypothesis is that SPNs in younger mice will be less complex as evinced most by dendritic arborization of SPNs. Following Purves and Lichtman's operational definition of dendritic complexity, in this study complexity will be measured by primary dendrite¹ number, dendritic length and branching (Purves and Lichtman, 1985). My hypothesis of increased complexity across development is supported by previous studies on guinea pigs finding increased dendritic length and increased number of primary dendrites across development in the celiac ganglion (Anderson, Jobling and Gibbins, 2001) and research in rats showing increased dendritic branching across development (Snider, 1988, Voyvodic, 1987a). Additionally, cell body size has been seen to increase during post-natal development in the superior cervical ganglia of cats and rats (Masliukov, 2001; Andrews, 1993). Thus, I expect to see that during development there is increased complexity of dendritic arborization, increased density of dendrites and a significant increase in soma size across neurons during development.

2. Materials and methods

2.1 Subjects

The mice I am using for this study are transgenic TH::Td mice, a strain of mice in which the chromophore tdtomato is inserted into the genome and expressed in a subset of tyrosine hydroxylase positive neurons (TH+). The value to having these transgenic mice is two-fold. Firstly,

¹ Although the term *dendrite* was used, un-branching dendrites could not be distinguished from axons. Therefore, neurites projecting outside of the ganglia were defined as axons and all other un-branching neurites were defined as dendrites.

around 95% of the neurons in the sympathetic chain ganglia are TH+, meaning they produce TH, a synthesis enzyme in the pathway for production of noradrenaline which is found in all of the noradrenergic neurons in the ganglia (See Figure 4).

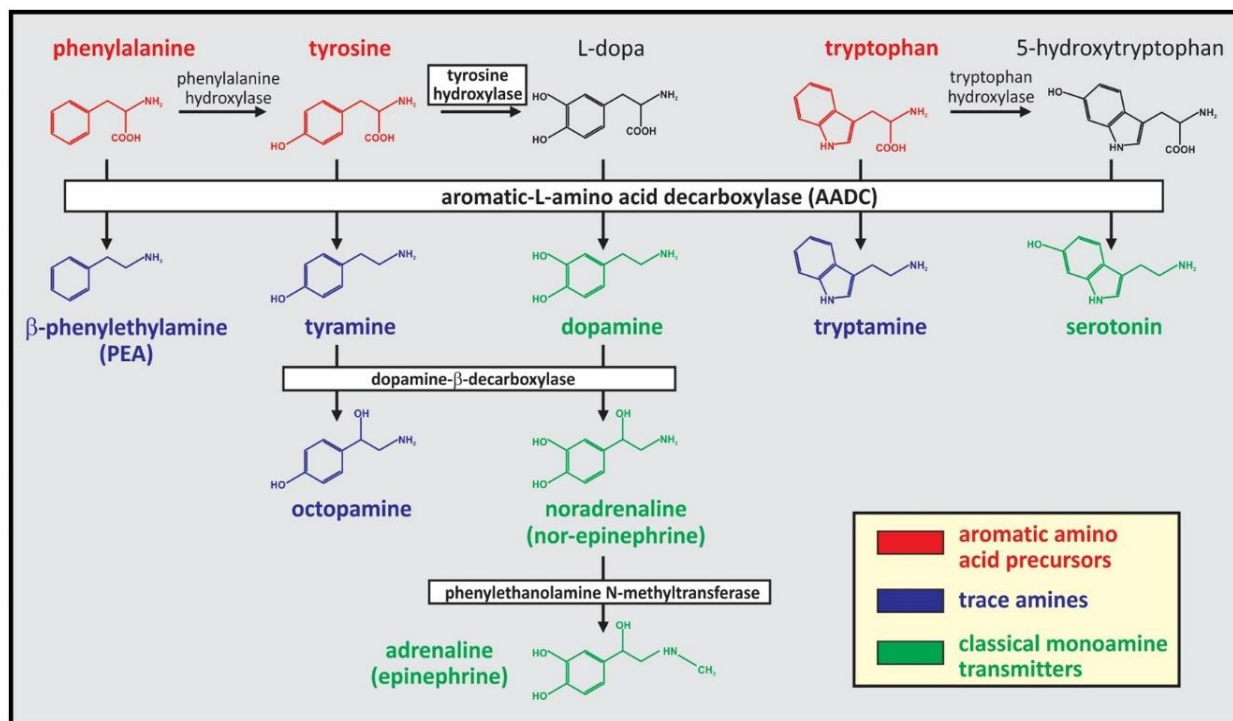


Figure 4: The monoamine synthesis pathways.

Relevant to this study, we can see how TH is necessary for the production of noradrenaline. Diagram adapted from Hochman, 2015

Therefore, I will study the type of neuron that comprises the majority of the T5 neuronal population. The second advantage comes from the nature of this label in that it allows for sparse cell specific Cre expression (Savitt et al., 2005). The mechanism for the sparseness is not entirely understood but the percent reporting is due to the amount of recombination of the reporter strain with the TH-Cre driver strain. Previous work done in the lab, specifically on neurons in the sensory system (dorsal root ganglia neurons), found the sparse label to be reporting around

8.33% of TH+ neurons (Watkins, 2018). This sparse label has been noted to label in a non-specific manner, without selection of neuronal subtypes (Badea et al., 2009; Watkins, 2018), therefore our sample should be random, non-stratified and representative of the noradrenergic population. The fact that label is sparse is critical for my study as this is the optimal situation for morphological analysis; label expressed in many neurons would preclude discrete reconstruction of individual thoracic SPNs due to dendrite density. The tissue will also be stained for TH by immunohistochemistry to visualize all TH+ in the ganglia in addition to the subset labeled by tdTomato. All tdTomato positive cells (Td+), following this, should be co-labelled with the TH antibody. In *Figure 5* and *6* the genetic tool is better explained. I will characterize SPN morphology in the fifth thoracic ganglion by age groups of post-natal days 21, 35 and 61-69 (3-4 mice will be studied at each time point).

Figure 5 : The Cre-Lox System

LoxP sites are inserted into the correct part of the genome for the creation of this transgene such that they flank the stop codon that stops the expression of the desired protein. To express the gene of interest, in this case tdTomato, the loxP-flanked stop codon must be excised. Cre cuts at these LoxP sites and allows for the transcription of the fluorescent marker thus, this tdTomato is only seen in Cre-expressing neurons. In these transgenic mice, Cre is expressed whenever TH is expressed thus the tdTomato marker stains for TH+ neurons. Diagram adapted from: Cre Lox Breeding for Beginners, Part 1. The Jackson Laboratory Available at: <https://www.jax.org/news-and-insights/jax-blog/2011/september/cre-lox-breeding> [Accessed March 28, 2020].

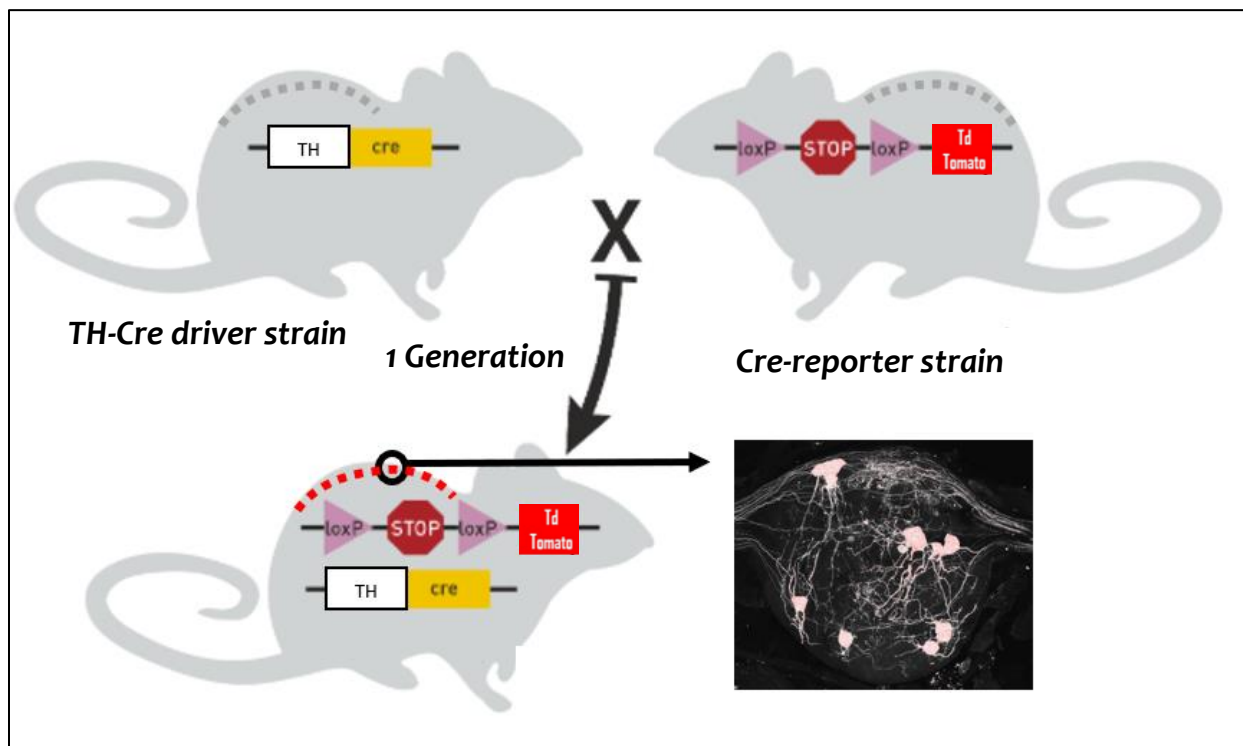
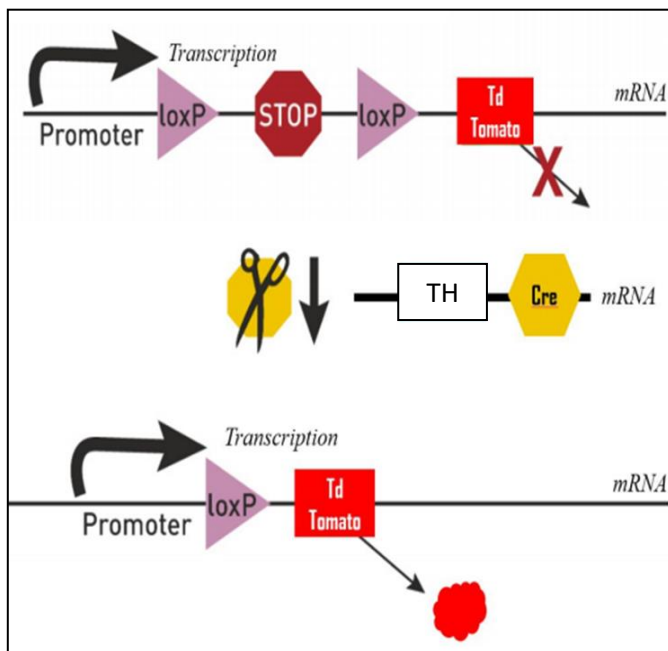


Figure 6: Genetic cross in TH::Td Transgenic mice

Here I show the cross that leads to the TH-Cre driver line in these transgenic mice. These mice are created by mating a TH-Cre driver strain with a Cre-reporter strain and so the marker is expressed in a subset of tissue with Cre activity only. The dotted lines represent the tSCG. Shown in the bottom right, is an image of T5 of an adult tdTomato transgenic mouse. This fluorescent marker tdTomato allows us to visualize the neurons and therefore our sample population consists exclusively of these labelled neurons. Diagram adapted from: Cre Lox Breeding for Beginners, Part 1. The Jackson Laboratory Available at: <https://www.jax.org/news-and-insights/jax-blog/2011/september/cre-lox-breeding> [Accessed March 28, 2020].

2.2 Age Categories: Developmental Aspect

The age categories are post-natal day (**PND**) 21, 35 and 60+. PND21 mice were collected just prior to weaning. The animal IDs are as follows for each individual PND21: PND21A, PND21B and PND21C. This pattern of naming was used to categorize animals in the PND 35 and PND 60+ age groups. Sexual development in mice has been seen starting at PND 35 (Lambert, 2009) so it was chosen as our adolescent group. PND60+ was chosen as our adult group, a characterization supported by research demonstrating that PND 60+ mice express adult levels of neurotransmitters (Romijn, et al., 1991) and synaptic density (Huttenlocher, 1979). Furthermore, the emergence of adult type behavior is seen in PND 60+ (Laviola, et al., 2003). In this way, we can study development just prior to weaning all the way up to adulthood with an intermediate point at a crucial stage in development, that is, sexual development and adolescence.

2.3 Tissue Preparation, Imaging and Tracing

All animals were transcardially perfused with 1/3 body weight:volume, 0.9% NaCl containing 10 units/ml heparin and 0.1% sodium nitrite followed by equal weight:volume 4 % paraformaldehyde, 0.1M phosphate (pH7.4). Following this, tissue was post-fixed in 4% paraformaldehyde, 0.1M phosphate (pH7.4) for 2 hours. Post-ganglionic chains were isolated and washed overnight in 0.1 M Phosphate buffered saline containing 0.3% triton-100 (PBS-T) at room temperature. Whole chains were then incubated in rabbit anti-RFP (Rockland Inc.) diluted to 1:100 and Sheep anti-TH (Millipore) diluted to 1:100 in PBS-T for 72-96 hours at 40°C. Whole chains were then washed 5 times per hour in PBS-T at room temperature followed by Cy3 conjugated donkey anti-rabbit (Jackson ImmunoResearch Laboratories Inc.) diluted to 1:250 and

Alexa-488 donkey anti-sheep (Jackson ImmunoResearch Laboratories Inc.) diluted to 1:100 in PBS-T for 24 to 48 hours at room temperature. Chains were then washed in PBS-T for 1 hour followed by another wash, 2 times per hour in 50mM Tris-HCl pH7.4 at room temperature. Chains were then placed on slides and cover-slipped with gold fade (Invitrogen) mounting media for visualization.

Table 2: Primary antibodies used for immunocytochemistry.

(TH = tyrosine hydroxylase, RFP = Red Fluorescent Protein). The tissues were incubated in these antibodies for 3-4 days at 40°C

PRIMARY ANTIBODY	HOST SPECIES	DILUTION	SOURCE
TH	Sheep	1:100	Millipore
RFP (RECOGNIZES TDTOMATO)	Rabbit	1:100	Rockland

Table 3: Secondary antibodies used for immunohistochemistry

(Cy3 = Cyanine 3). The ganglia were incubated in these antibodies for 24-48 hours at room temperature

SECONDARY ANTIBODY	DILUTION	SOURCE
CYTM3 DONKEY ANTI-RABBIT	1:250	Jackson
ALEXA FLUOR[®] 488 DONKEY ANTI-SHEEP	1:100	Jackson

All animals were males, apart from one PND 21 (PND21A), whose sex was not documented. Both left and right sympathetic chain ganglia are present in the mouse, however, this parameter was not recorded in this research and thus the sidedness of the T5 ganglia was not n accounted for. In a study on the cat stellate ganglion, Masliukov (2001) noted some right-left differences in morphological features but these were not constant in different ages. In particular, apart from newborn kittens, ganglion cell number did not differ between left and right. T5 was our chosen thoracic ganglion because it is easily identifiable, large enough that sufficient number of neurons will be stained in our sparse label model and relatively small such that tSPN reconstruction is feasible. Furthermore, T5 innervates various different tissues dispersed throughout the body (see *Table 4*) so studying SPNs in T5 allows us to better understand general

sympathetic nervous system organization and not just organization as it relates to one organ system.

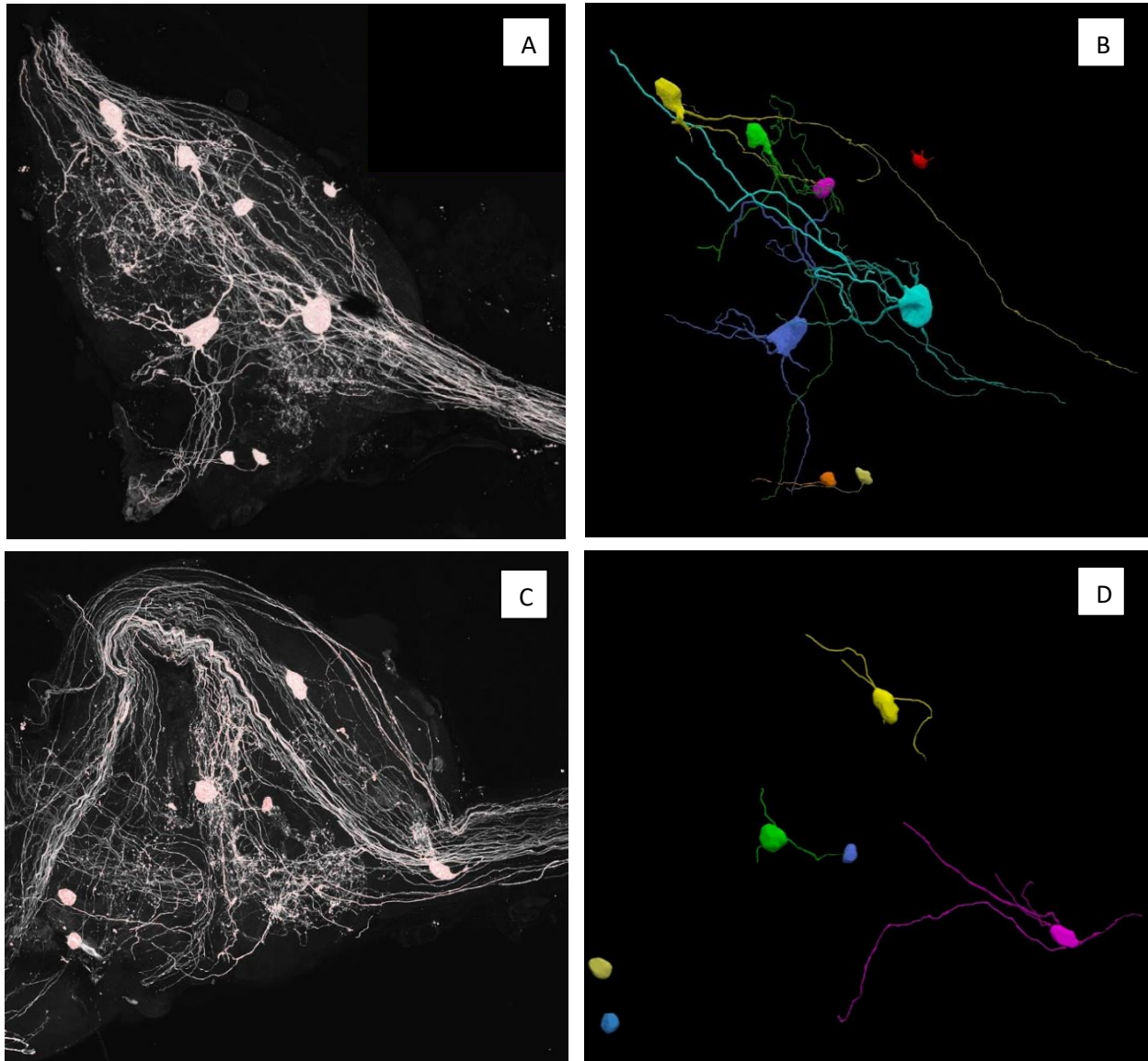


Figure 7: Confocal Images and Reconstructions

A. Confocal image of T5 of PND61A. As seen in this image, the only neurons visualized are those with the red-fluorescent tdTomato stain, representing a small population of the TH+ (noradrenergic) neurons in the ganglion.

B. This image shows a reconstruction done in NL360. In this example, all dendrites were reconstructed, rather than only primary dendrites for a more complete visualization of dendritic organization. The reconstructions allow for the extraction of data relating to soma volume and surface area, dendrite length, branching patterns amongst other data points that the software provides.

C. Another example of an imaged ganglion in these transgenic mice. This is T5 of PND63D

D. Full reconstruction of T5 of PND63D

Sparse labeling of the entire ganglion was imaged on an Olympus Fluoview 1000 confocal microscope for morphological reconstruction of individual SPNs (60x, oil, 1.25 NA, 0.46-0.51 μ m Z-steps). Examples of two T5 ganglia from the PND 60+ adult population are shown (see Figure 7). Composite images comprising each ganglion were analyzed in NeuroLucida 360 software (MBF Bioscience, Williston, VT) and cell bodies and dendrites of Td+ neurons were reconstructed using both user-guided and manual modes. Reconstructions were quantified with Neuroexplorer software (MBF Bioscience, Williston, VT) to obtain data on individual neurons including soma volume, number of dendrites, primary dendrite length and mode of termination. A primary dendrite for the purposes of this study was operationally defined as any process that extends from the soma for more than a distance of 2 μ m, a definition adapted from Snider, 1986.

Even with confocal images, the entire pattern of dendrite branching was hard to reconstruct with accuracy as the smaller more distant arbors were at times unclear. For this reason, reconstructions of dendrites consisted of only the primary process, of which I had the maximum certainty. For primary dendrites that branched, terminal length was recorded as the first point of branching (i.e., the first node). Un-branching primary dendrites were traced until their termination. As SPNs project axons outside their ganglion, un-branching dendrites were defined as those that end within the T5 ganglion. Axonal projections were excluded from the analysis since their full length could not be determined. If a primary dendrite bifurcated, a 'node' as termed by the software was placed at the end signaling branching, whereas a primary dendrite with no nodes simply was terminated on an 'ending' as defined by the software (see *Figure 8*). In this way, branching dendrites were differentiated from un-branching dendrites and measures of their relative incidence and length were compared within and between age groups. Dendrograms

were constructed for the PND 60+ population (Figure 7) but are not presented in this thesis of SPN development.

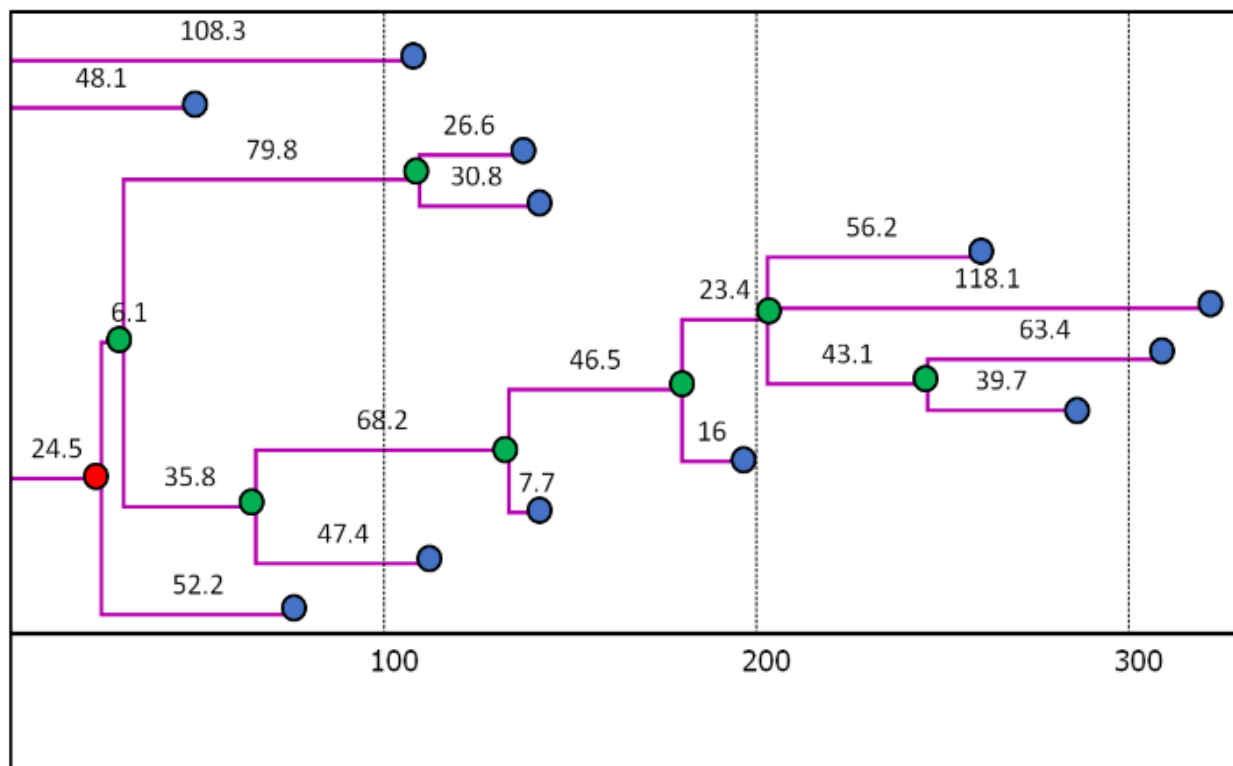


Figure 8: Dendrogram of a Sympathetic neuron

This shows the dendritic arborization of a neuron in a PND 60+ mouse T5. Red dots are primary nodes, green dots are non-primary nodes and blue dots are endings. The x axis is primary dendrite length in μm . From top to bottom, dendrite #1 and #2 would be classified as un-branched primary dendrites with a length of $108.3\mu\text{m}$ and $48.1\mu\text{m}$ respectively while dendrite #3 would be recorded as a branched dendrite with a length of $24.5\mu\text{m}$.

2.4 Data Analysis

All values are presented as mean \pm the standard deviation unless stated otherwise. A Normality Test (Shapiro-Wilk) and an Equal Variance Test (Brown-Forsythe) was conducted to determine which statistical test to use. A Kruskal-Wallis H test, also called a one-way analysis of variance (ANOVA) on ranks, was used to compare data sets with a dependent continuous variable

and an independent categorical variable. Thus, a one-way ANOVA was run on number of neurons, number of dendrites, cell body volume and dendritic length to test the equality of morphological parameters within and between age groups. ANOVA results cannot determine which difference between pairs of means drives the significance. Thus, to isolate the group or groups that differ from each other an all Pairwise Multiple Comparison Procedure was used, also known as Dunn's Method.

A Chi-square statistic was run to compare data sets consisting of a categorical independent and dependent variable such as branching of primary dendrites. Yates continuity correction option was not applied to calculations. Again, this was done both to test variation within and between developmental age groups. Data analysis was performed using the SigmaPlot software.

3. Results

3.1 *Neuron Number Across Development*

Literature suggests that neuron number is not constant during ontogenesis. The mean number of Td+ sparse-labeled neurons across the 3-4 ganglia analysed for PND 21, PND 35 and PND 60+ are 29.7 ± 12.8 , 21.7 ± 12.5 and 17.8 ± 15.9 respectively. Numbers are not significantly different between age groups ($p = 0.57$; power = 0.05; one-way ANOVA). However, as seen in *Figure 9*, the number of sparse labeled neurons in the T5 ganglia of mice in any age group is highly variable, making the sample underpowered. As the sparse labeling approach is stochastic, a possible explanation for this variability is that labeled neuron numbers may not be consistently expressed in the same fraction of total neurons within ganglia of individual mice.

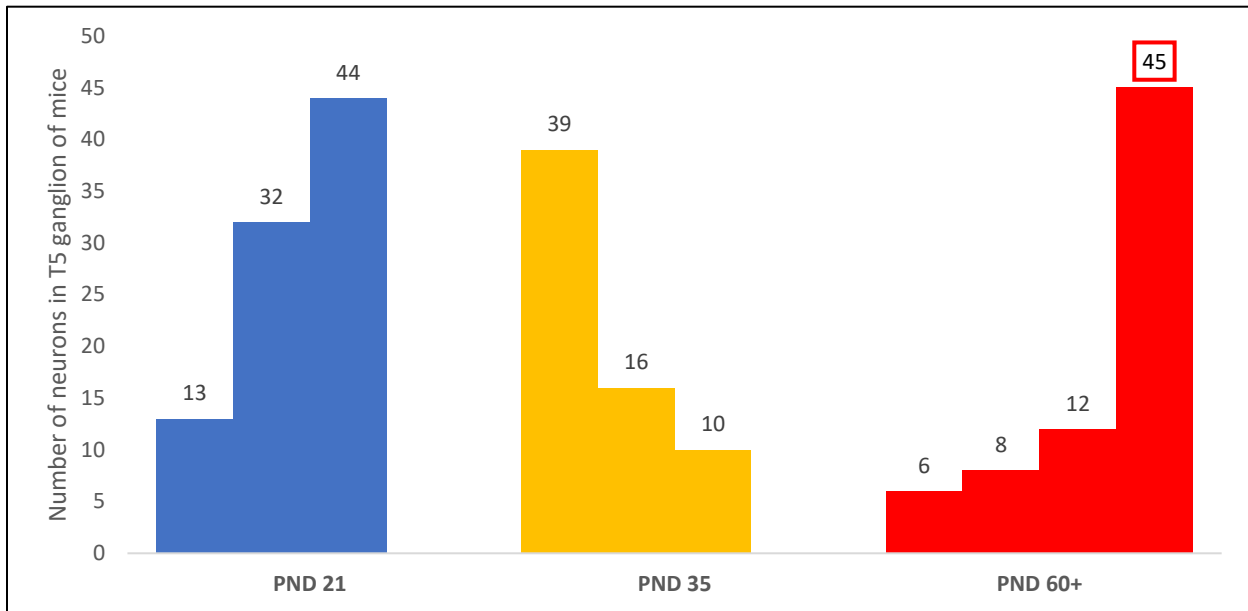


Figure 9: Raw Td+ neuron counts in T5 ganglia at three developmental stages.

Each bar represents the population in a single T5 ganglia of a single mouse. A significant outlier determined by the Grubb's test is boxed ($p < 0.05$). The differences in the mean values among the treatment groups are not great enough to exclude the possibility that the difference is due to random sampling variability; there is not a statistically significant difference ($p = 0.57$). If this outlier is then removed, the average number of neurons in the T5 ganglia across development is still not significantly different at a 95% CI ($p = 0.1$)

3.2 Primary Dendrite Number Across Development

Previous studies on development of dendrites in cervical ganglia in rats have been conflicting showing either increases, decreases or no change in the number of primary dendrites across development (Andrews, 1993, Snider, 1988, Voyvodic, 1987a; Anderson et al., 2001). Part of this variability may relate to study differences in the age range examined. In general there is consensus that dendritic complexity increases during development. The increase in complexity is accounted for mostly by an increase in dendritic length and branching (Purves et al., 1986). To get a rough understanding of dendritic arborization, I counted the number of primary dendrites emanating from the soma. These included un-branching dendrites and branching dendrites (i.e., ending in a bifurcation).

The number of primary dendrites per neuron was 5.0 ± 2.7 , 3.0 ± 2.3 and 3.7 ± 2.5 across the T5 ganglia analyzed for PND 21, PND 35 and PND 60+, respectively. The difference in the median values amongst the different age groups was significant ($p < 0.001$; one-way ANOVA on Ranks). Pairwise Comparison showed that only PND 21 versus PND 35 groups differed significantly ($p < 0.001$; Dunn's Method).

Table 4: Descriptive statistics of number of primary dendrites per neuron

There seems to be some variability in average number of dendrites per neuron amongst individuals of the same age, particularly in adulthood.

	PND 21			
ANIMAL ID	<i>PND21A</i>	<i>PND21B</i>	<i>PND21C</i>	
AVERAGE NUMBER OF PN PER NEURON	5.85	4.87	4.82	
STANDARD DEVIATION	2.71	2.42	2.88	
OVERALL NUMBER OF PN PER NEURON IN PND 21	5.0 ± 2.7			
	PND 35			
ANIMAL ID	<i>PND35A</i>	<i>PND35B</i>	<i>PND35C</i>	
AVERAGE NUMBER OF PN PER NEURON	2.82	5.86	1.5	
STANDARD DEVIATION	2.33	1.77	2.91	
OVERALL NUMBER OF PN PER NEURON IN PND 21	3.0 ± 2.3			
	PND60+			
ANIMAL ID	<i>PND63D</i>	<i>PND61A</i>	<i>PND61B</i>	<i>PND69C</i>
AVERAGE NUMBER OF PN PER NEURON	1.83	2.88	4.67	3.86
STANDARD DEVIATION	1.95	2.52	2.46	1.77
OVERALL NUMBER OF PN PER NEURON IN PND 21	3.7 ± 2.5			

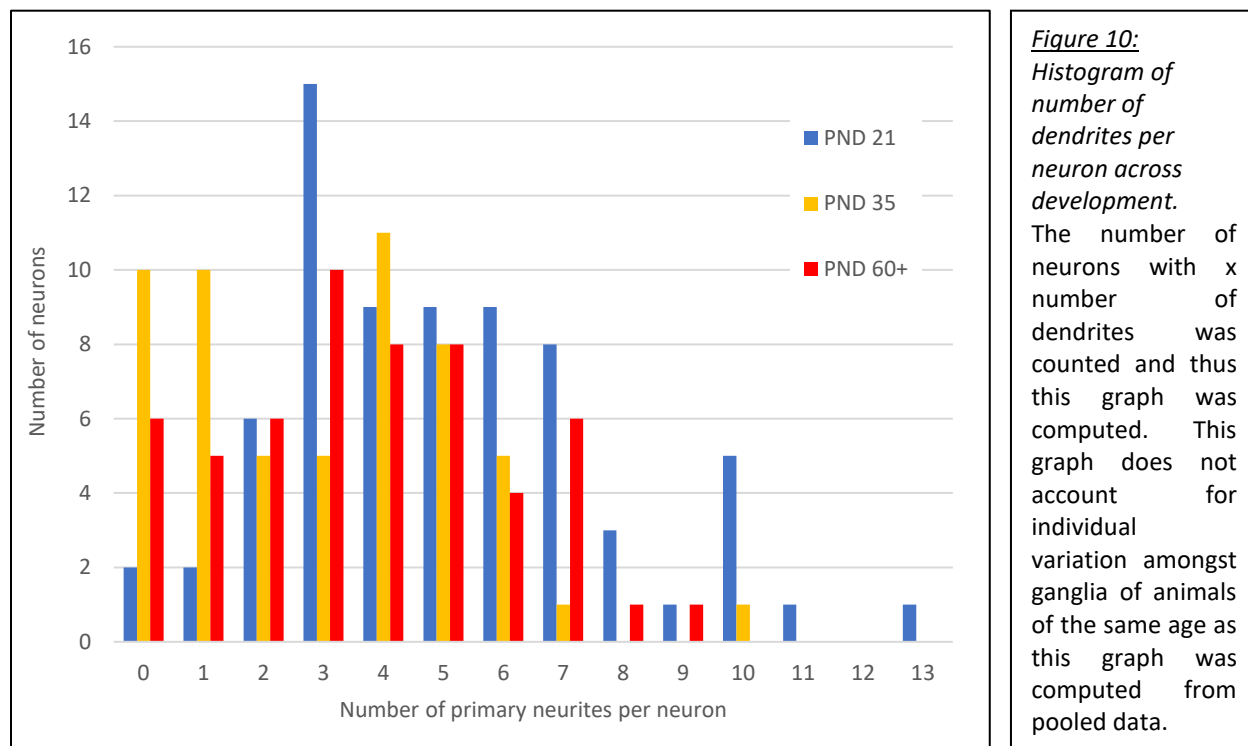


Table 4 presents mean values of primary dendrite number per neuron between and within age groups. Significant difference in number was seen between ganglia of mice at PND 35 and at PND 60+ (both at $p < 0.05$; one-way ANOVA). Observed individual variability at later ages may be an important factor in evaluating factors affecting plasticity in dendritic arborization post-weaning.

3.3 Comparing Incidence of Primary Dendrite Branching Across Development

Literature suggests increased dendritic complexity during development (see Table 1). I observed both branching and un-branching dendrites and sought to compare their incidence during development.

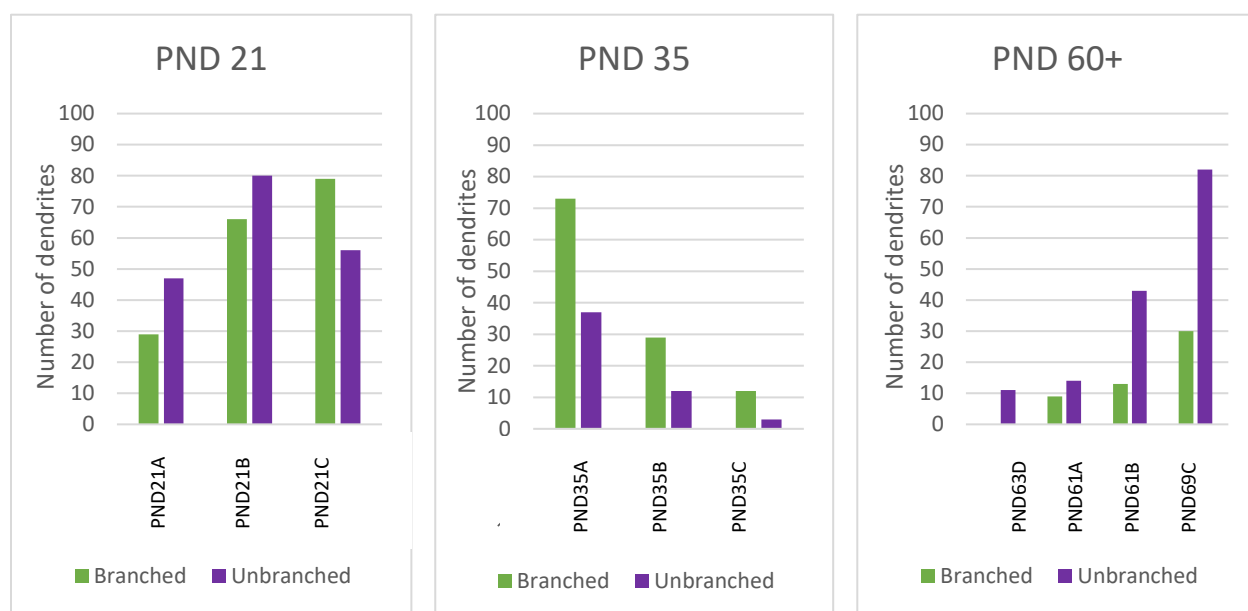


Figure 11: Comparing incidence of branched and un-branched dendrites between ganglia in individual mice.

The majority of dendrites in each ganglia in PND 21 were un-branched, although the split between branched and un-branched was fairly even at this age point for all animals. Most dendrites in PND 35 mice were branched in all ganglia. In contrast most dendrites in PND 60+ mice were un-branched.

There were significant differences in the incidence of branched and un-branched dendrites between all age groups (all at $p < 0.001$; Chi-square test). Interestingly, inter-animal differences were seen in ganglia from the youngest mice (PND 21; $p=0.01$) but not for PND 35 ($p=0.54$) or PND 60+ mice ($p=0.35$). Numerical values can be seen in *Table 5* and trends within and between age groups can be seen in *Figure 11*.

Table 5: Descriptive statistics of branching data in neurons

PD=primary dendrite

	PND 21	PND 35	PND60+
NUMBER OF BRANCHED DENDRITES	174	114	52
NUMBER OF UN-BRANCHED DENDRITES	183	52	150
TOTAL NUMBER OF DENDRITES	71	56	54
% BRANCHED	48.7	68.7	25.7
AVERAGE NUMBER OF PDs PER NEURON	5.03	2.96	3.67
STANDARD DEVIATION	2.69	2.27	2.54

3.4 Comparing Dendrite Length Across Development

As Td+ neurons generally contained branched and un-branched dendrites I assessed whether their lengths changed during development. At all age groups, un-branched dendrites were longer than primary dendrite lengths of branching dendrites ($p < 0.001$ at PND21 and PND60+; $p < 0.01$ for P35; Mann-Whitney Rank Sum Test). These differences were even significant in 6 of 9 individual ganglia tested (Welch's t-test; See *Table 6*).

Table 6: Difference between branching and un-branching dendrite length in individual mice T5 ganglia

Age group	Animal ID	P value between branching and un-branching dendrite length	Significant? (p<0.05)
PND21	PND21A	<0.001	YES
	PND21B	<0.0001	YES
	PND21C	0.07	NO
PND35	PND35A	<0.01	YES
	PND35B	0.78	NO
	PND35C	<0.05	YES
PND 60+	PND61A	0.81	NO
	PND61B	<0.01	YES
	PND69C	<0.0001	YES

Therefore, statistical tests were separately conducted to assess age-related length differences in primary dendrite length of branching dendrites and un-branched dendrites. Primary dendrite length of branching dendrites differed significantly between age groups ($p < 0.001$; Kruskal-Wallis One Way ANOVA on Ranks). Pairwise Comparison (Dunn's Method) showed that significance was due to significantly shorter lengths at PND21 compared to PND35 or PND60+ ($p < 0.001$) whereas PND35 and PND60+ lengths were similar ($p = 0.7$). Mean length values increased with age (See *Table 7*).

Similarly, the length of un-branching dendrites differed between age groups ($p < 0.001$; Kruskal-Wallis One Way ANOVA on Ranks). Pairwise Comparison (Dunn's Method) showed that

un-branching dendrites were longer in the adult PND60+ population than those at PND21 and PND35 ($p < 0.001$ and $p=0.002$, respectively) while PND21 and PND35 lengths were similar ($p = 0.7$). Mean length values increased numerically with age (See *Table 7*).

Table 7: Descriptive statistics on branched vs. un-branched primary dendrite length

Age (n)	Neuron number	Dendrite measured	Total # dendrites	% of dendrites branching	Mean Length \pm SD (μm)
PND21 (3)	89	Branching	173	48.3	21.6 \pm 23.1
		Un-branching	185		34.0 \pm 27.6
PND35 (3)	65	Branching	114	68.7	28.2 \pm 21.8
		Un-branching	52		41.8 \pm 38.1
PND60+ (4)	71	Branching	52	25.7	36.8 \pm 35.7
		Un-branching	150		76.3 \pm 70.9

Interestingly, while primary dendrite length of branching dendrites was similar between mice of the same age group at PND35 and at PND60+, length between mice at PND21 differed significantly ($p < 0.001$; Kruskal-Wallis One Way ANOVA on Ranks). In comparison, no differences were seen in un-branching dendrite lengths between mice within each age group (Kruskal-Wallis One Way ANOVA on Ranks). As described above, Td+ neurons generally contained branched and un-branched dendrites and these proportions differed between mice from the different ages sampled.

Graphical presentation of these differences between ages and within individual age groups are presented as histograms (*Figure 12*), cumulative sum distributions (*Figure 13*) and Box and Whisler plots (*Figure 14*). Further details are provided in their respective legends.

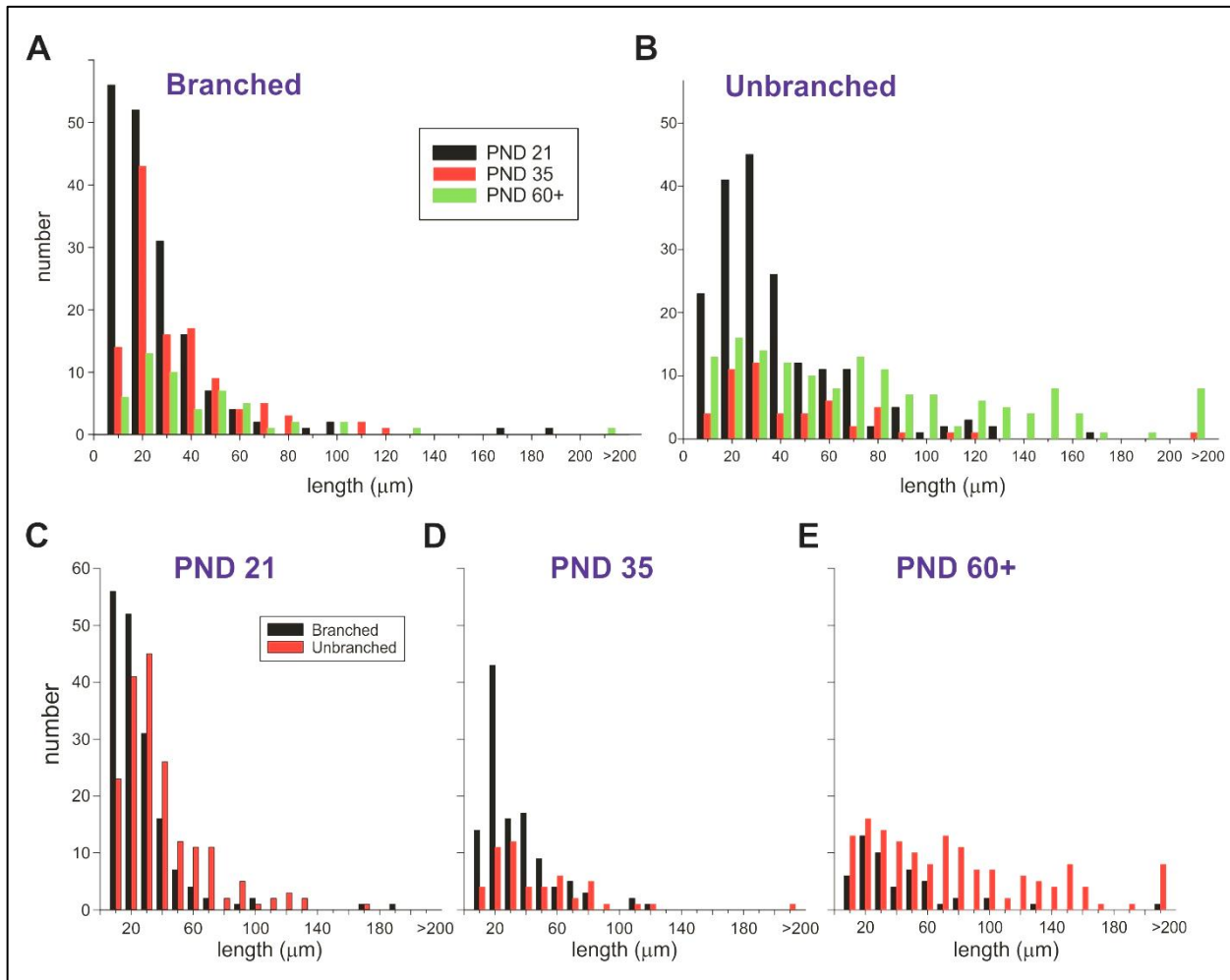


Figure 12: (A-E) Histograms showing distribution of branched and un-branched primary dendrite length across development

A and **B** show distribution of branched and un-branched primary dendrite length respectively. Of note, the majority of PND 21 branched and un-branched dendrites lie in the 0μm-40μm category (89.0%, 73.0% respectively). This range makes up 79.0% and 63.5% of branched dendrites and 60.0% and 36.4% of unbranched PND 35 and PND 60+ dendrites respectively. Mean un-branched primary dendrite length was greatest in PND 60+ and this can be seen in graph B showing the majority of un-branched dendrites longer than 120μm are of PND60+ mice.

C-E show the distribution of branched and un-branched dendrites in each age group plotted against length. As can be seen, the length of un-branched dendrites is significantly greater in all age groups, particularly PND 60+. Furthermore, we can also see how the raw number of dendrites decreases across development, with a predominant loss of shorter dendrites.

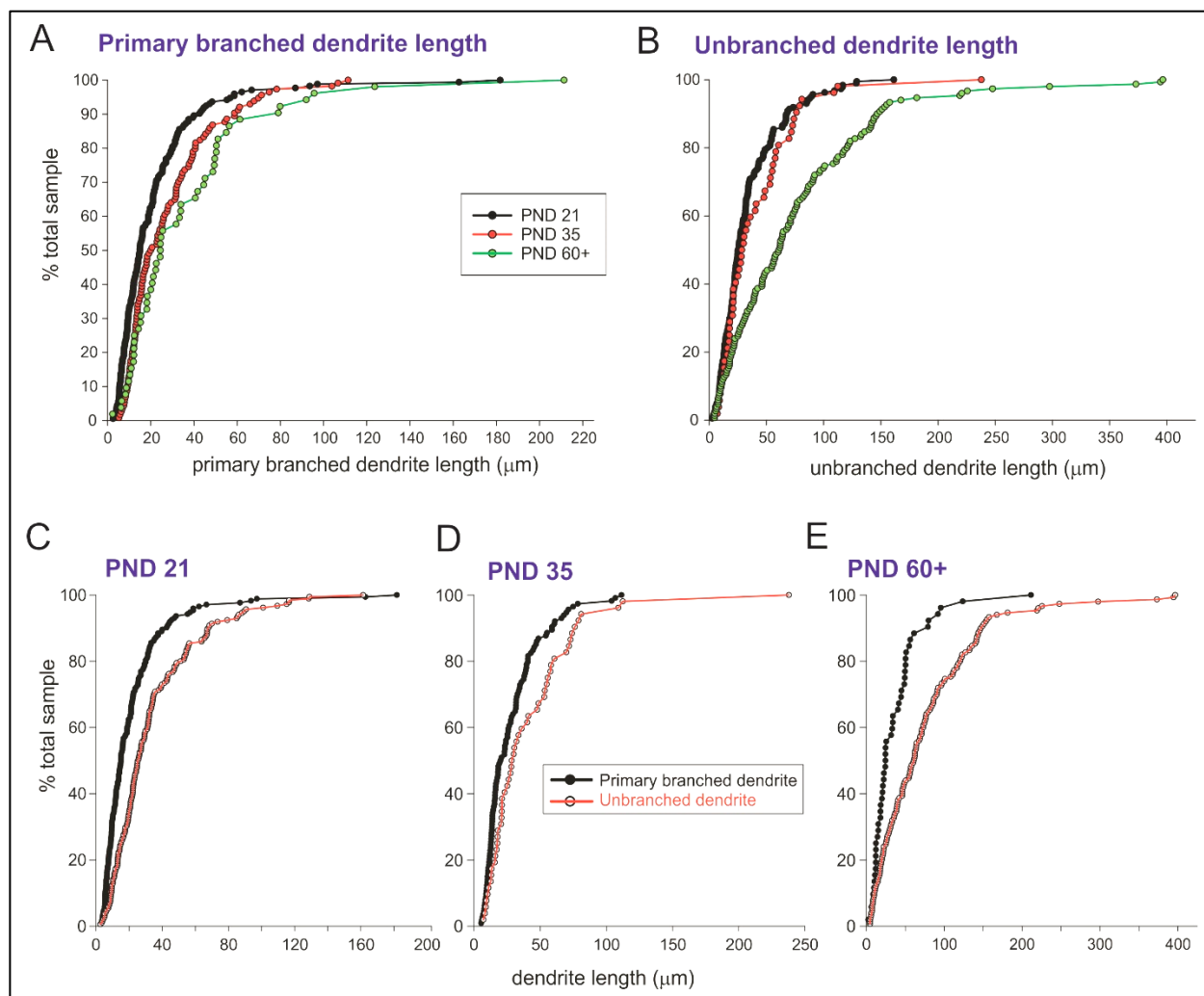


Figure 13: (A-E): Cumulative sum graphs for branched and un-branched dendrite length

The numbers here are normalized to 100% of the sample. 12.A and 12.B show un-branched and branched primary dendrite lengths for all age groups for comparison. Notably, PND 60+ mice have the largest amount of dendrites with the longest lengths. Graphs 12.C, 12.D and 12.E show differences between branched and un-branched dendrite lengths in each age category after pooling all dendrite lengths across the ganglia in that age group.

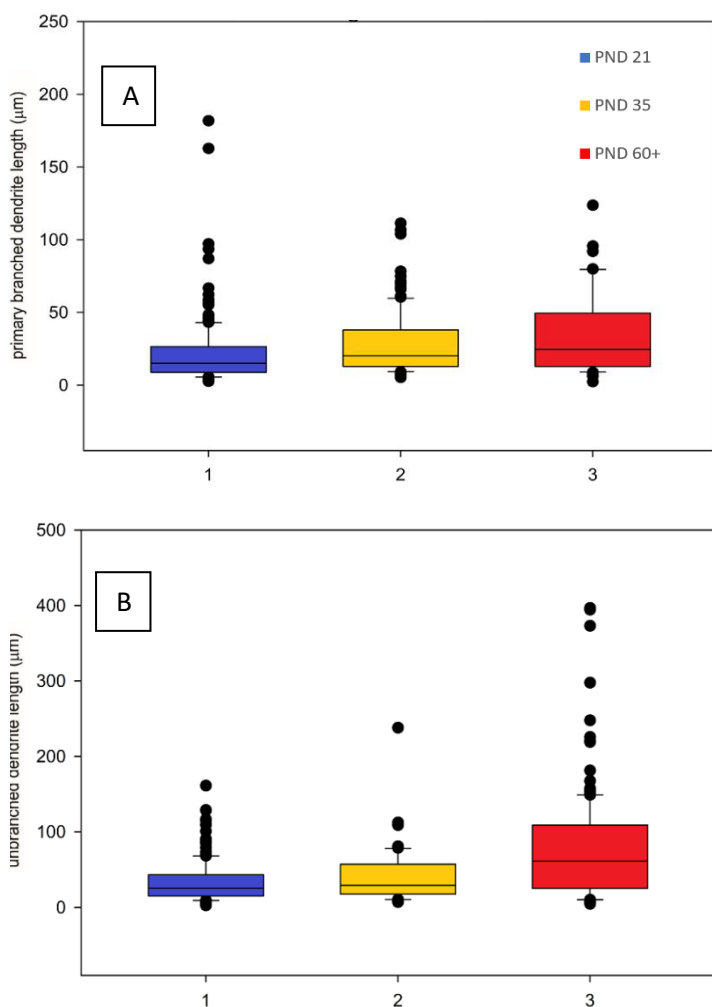


Figure 14: (A-B) Box and Whisker Plots for branched and un-branched primary dendrite length across development

A. Distribution of length of branched primary dendrite in the different age categories studied.

B. Un-branched primary dendrite length.

In these graphs we can see spread of dendrite length across development. The PND 60+ group has some particularly long un-branched dendrites.

3.4 Cell Body Volume Across Development

Studies done on rats suggests a different time course for somatic growth compared to dendritic growth (Anderson et al., , 2001; Nunez-Abades and Cameron, 1995). In multiple studies of sympathetic ganglia neuronal size increases during post-natal ontogenesis (Masliukov, 2001; Andrews, 1993; Voyvodic, 1987a). Cell body size is an important morphological measure and can be related to cell metabolic and recruitment properties. Below I compared several features of SPN soma size across development, with focus on cell volume.

In my study of the T5 ganglia in mice, the cell body volumes for PND 21, PND 35 and PND 60+ were $1575\mu\text{m}^3 \pm 932\mu\text{m}^3$, $1957 \pm 1696\mu\text{m}^3$ and $1906\mu\text{m}^3 \pm 1121\mu\text{m}^3$, respectively. As Figure 15 and Table 8 show, PND 35 had the largest range for cell body volume ($7267 \mu\text{m}^3$).

Table 8: Descriptive statistics on cell body volume across development

	SIZE	MEAN	MEDIAN	STD DEV	MAX	MIN	RANGE
PND 21	71	1575.365	1390.88	938.343	4772.99	349	4423.99
PND 35	56	1956.858	1320.93	1711.742	7533.94	267.12	7266.82
PND 60+	53	1905.817	1750	1131.962	5578.51	411.81	5166.7

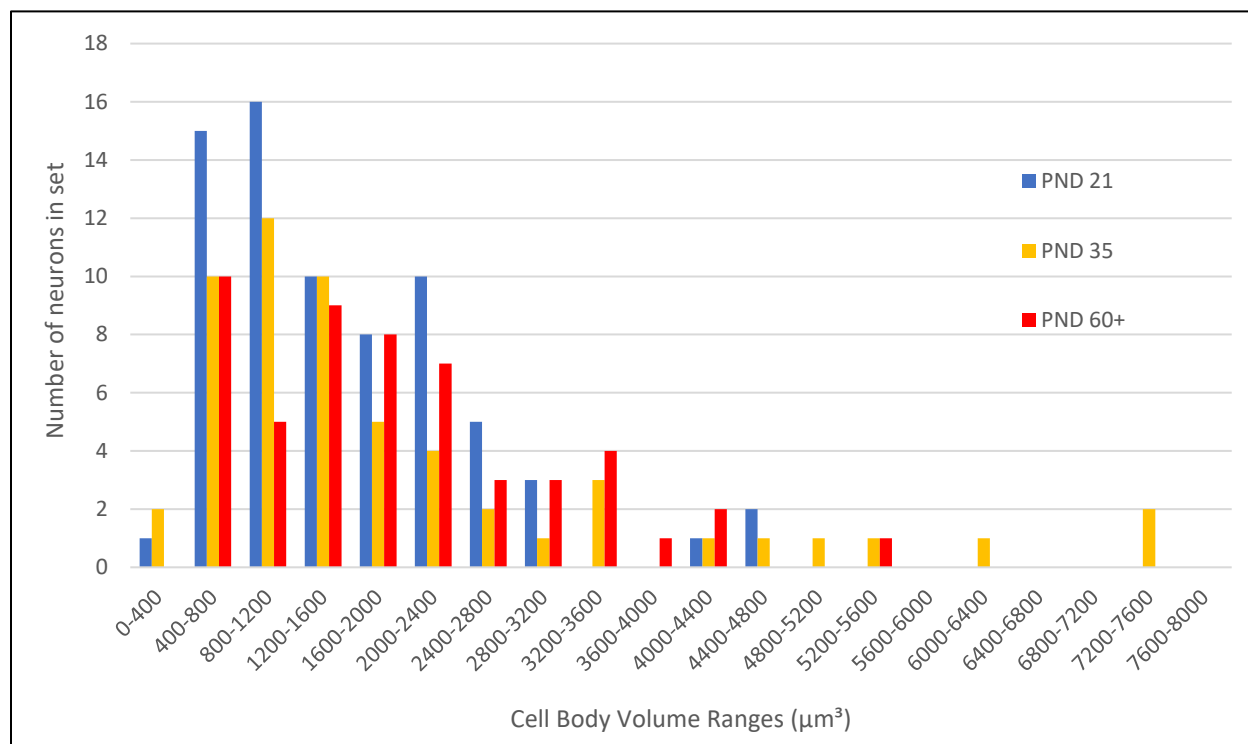


Figure 15: Histogram of cell body volume across development.

The data here is pooled by age group. Distribution was done for size groups in increments of $400\mu\text{m}^3$ by counting how many cells in the T5 of all PND 21, PND 35 or PND 60+ mice fell in that range. For all developmental ages, the majority of neurons had soma volumes in the range of $400\mu\text{m}^3$ - $1600\mu\text{m}^3$. No cells smaller than $400\mu\text{m}^3$ were found in PND 60+ and no cells larger than $4800\mu\text{m}^3$ were found in PND 21s. PND35s had the largest range having the cell with the smallest soma size ($267.1\mu\text{m}^3$) and largest soma size ($7533.9 \mu\text{m}^3$) of all neurons analyzed for this study. Furthermore, the distribution in all age groups does not seem to be bell-shaped, but instead skewed.

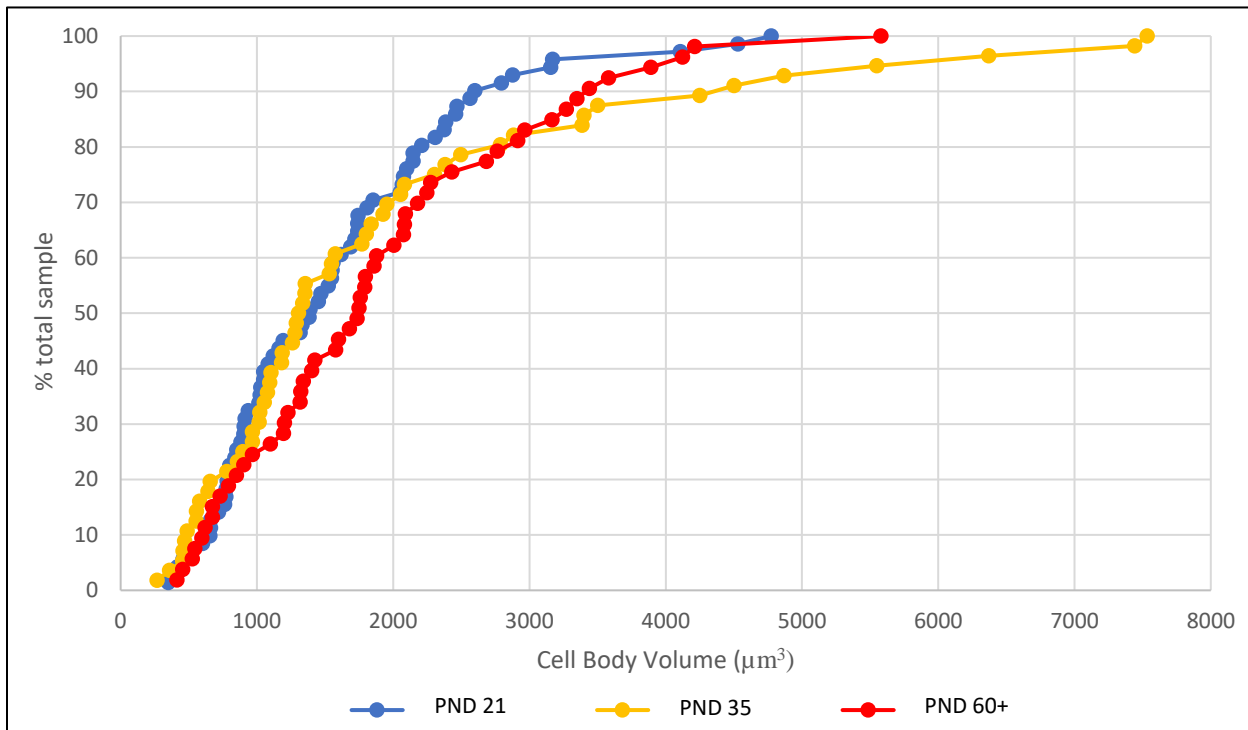


Figure 16: Cumulative sum graph of cell body volume across development

This line graph shows all cell body volume data points organized from smallest to largest by age group normalized to 100% of the sample

Differences in the mean values were not significantly different ($p=0.18$; a one-way ANOVA).

Figure 16 shows the cumulative sum distribution of cell volume of the three age groups to further visualize their lack of overt difference. Individual differences of cell volumes obtained are shown as Box and Whisker plots in *Figure 17*. For within-group comparison, significant differences are seen in cell body volume populations between animals at PND 21 ($p<0.001$) and PND 60+ ($p<0.05$) but not PND 35 ($p=0.26$; one-way ANOVA). This suggests that individual differences overpower developmental ones concerning cell size.

For some cells maximal cross-sectional area was determined manually; because of their proximity to each other, reconstruction software could not determine the volume for 22.2%,

3.8% and 22.5% of Td+ neurons in PND 21, PND 35 and PND 60+ respectively. For these neurons, reconstruction of primary dendrites was also not conducted.

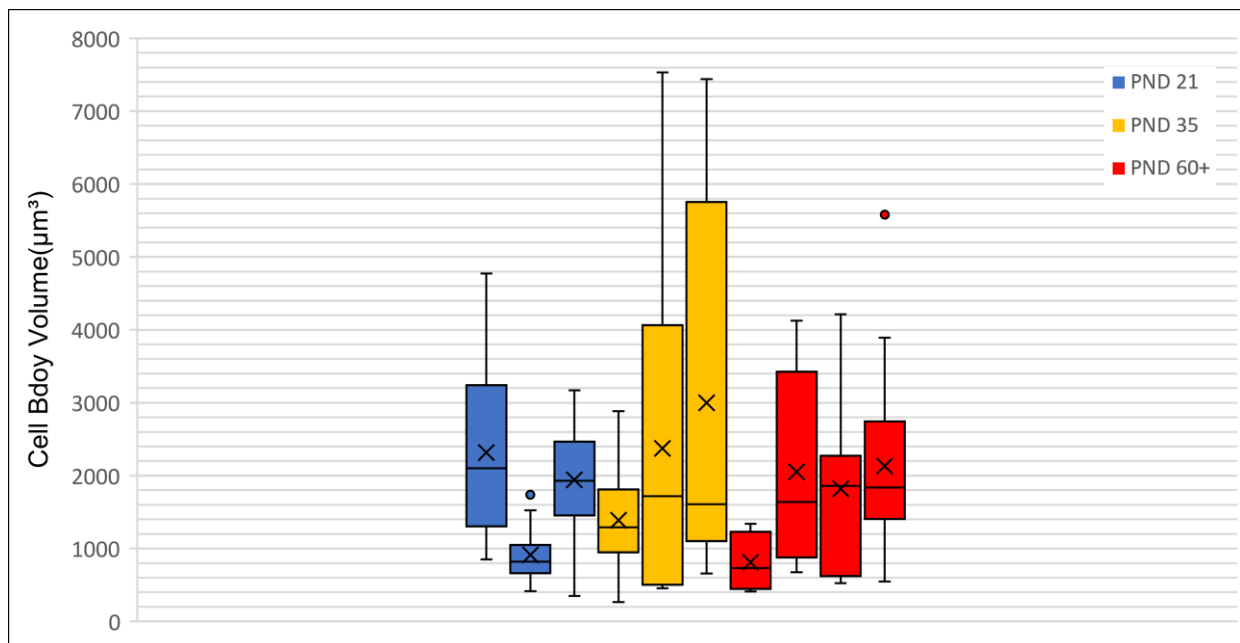


Figure 17: Box and Whisker plots for cell body volumes across development

Each box and whisker plot represents neuron volume values for neurons in the T5 tSCG of an individual mouse.

Cross-sectional area (CSA) has been a popular parameter in the literature to measure cell size and has been seen to increase in post-natal development. Here I contoured cell bodies for which volumetric reconstruction could not be undertaken by selecting the Z-level at which soma size was the largest. Note that these values therefore do not reflect the same population from which volume measures were obtained. Our results for these cells show that the average CSA for PND 21, PND 35 and PND 60+ was $208\mu\text{m}^2 \pm 81\mu\text{m}^2$, $269\mu\text{m}^2 \pm 70\mu\text{m}^2$ and $357\mu\text{m}^2 \pm 214\mu\text{m}^2$ respectively demonstrating a post-natal increase. For CSA a one-way ANOVA showed that the difference across development was statistically significant ($p=0.02$). By Dunn's Method the two groups that vary the greatest in area compared to each other are PND 21 and PND 60+. The

average perimeter was $74.7\mu\text{m} \pm 50.0\mu\text{m}$, $64.7\mu\text{m} \pm 9.6\mu\text{m}$ and $74.5\mu\text{m} \pm 24.1\mu\text{m}$ for PND 21, PND 35 and PND 60+ respectively. Maximum perimeter data following a one-way ANOVA did not show a significant difference across development for the three age groups ($p=0.19$).

Table 9: Descriptive statistics of Contour data

	PND 21		PND 35		PND 60+	
	Perimeter(μm)	Area(μm^2)	Perimeter(μm)	Area(μm^2)	Perimeter(μm)	Area(μm^2)
	61.52	207.36	61.53	255.18	69	291.61
	54.64	191.77	49.73	187.47	60.41	
	60.2	205.13	63.92	301.88	34.06	68.79
	68.94	257.29	78.17	367.74	35.71	93.1
	66.04	291.05	65.11	231.83	81.37	325.57
	45.66	147.58	51.74	186.06	74.27	372.24
	55.36	204.91	63.11	195.81	81.29	334.07
	69.61	292.88	69.55	349.3	67.41	328.89
	58.35	232.24	79.39	341.97	72.12	341.06
	55.92	191.64			101.95	567.82
	56.28	208.38			98.31	490.68
	35.63	88.1			91.34	505.72
	63.72	251.52			133.47	1005.86
	56.43	214.8			72.51	343.23
	93.79	389.58			69.41	258.48
	65.37	251.85			48.95	151.95
	106.63	42.05				
	270.7	73.78				
Average	74.7	207.9	64.7	268.6	74.5	356.9
Standard Deviation	50.0	81.0	9.58	69.2	24.1	214.0

3.5 Rostro-caudal Analysis

For 3 adults (PND63D, PND69C, PND69E), Td+ cells in T4, T5, T6 and T7 were counted to evaluate rostro-caudal differences in the tSCG of mice. T4 was not available for PND63D. For this rostro-caudal study images were obtained as a single projection and collected on a Keyence or Nikon Microscope set to x20 magnification. The images were uploaded onto NeuroLucida and Td+

cells were marked and then counted using NeuroExplorer. Counting was done twice for accuracy and reproducibility, and the number reported is the average of these two counts.

The purpose of my rostro-caudal analysis was two-fold. Firstly, to see whether neuron morphology changes between rostral versus caudal ganglia as has been noted previously in literature (Snider, 1986; Jobling and Gibbins, 1999). The second purpose of this qualitative look at T4-T7 was to see whether differences between individuals in Td+ neuron number would be maintained across different ganglia. Looking at *Figure 18*, we can see that for any given ganglia the number of neurons in PND69C > PND69E > PND63D. A one-way ANOVA revealed a significant difference amongst Td+ populations in ganglia of different adults at a 95% CI ($p=0.0012$). Further to this point, a one-way ANOVA of T5, T6 and T7 Td+ populations reported no statistically significant difference ($p=0.79$) amongst the groups.

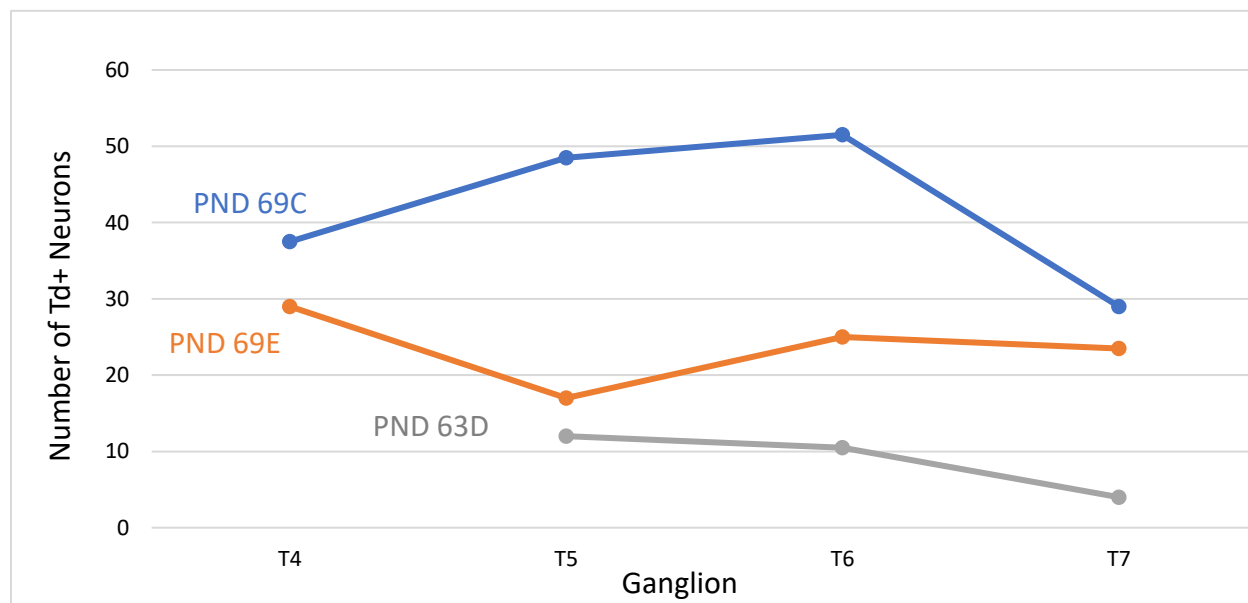


Figure 18: Rostrocaudal differences in number of Td+ neurons

No clear trend is seen other than that the numbers are not constant throughout this section of the tSCG in the same animal even in adulthood.

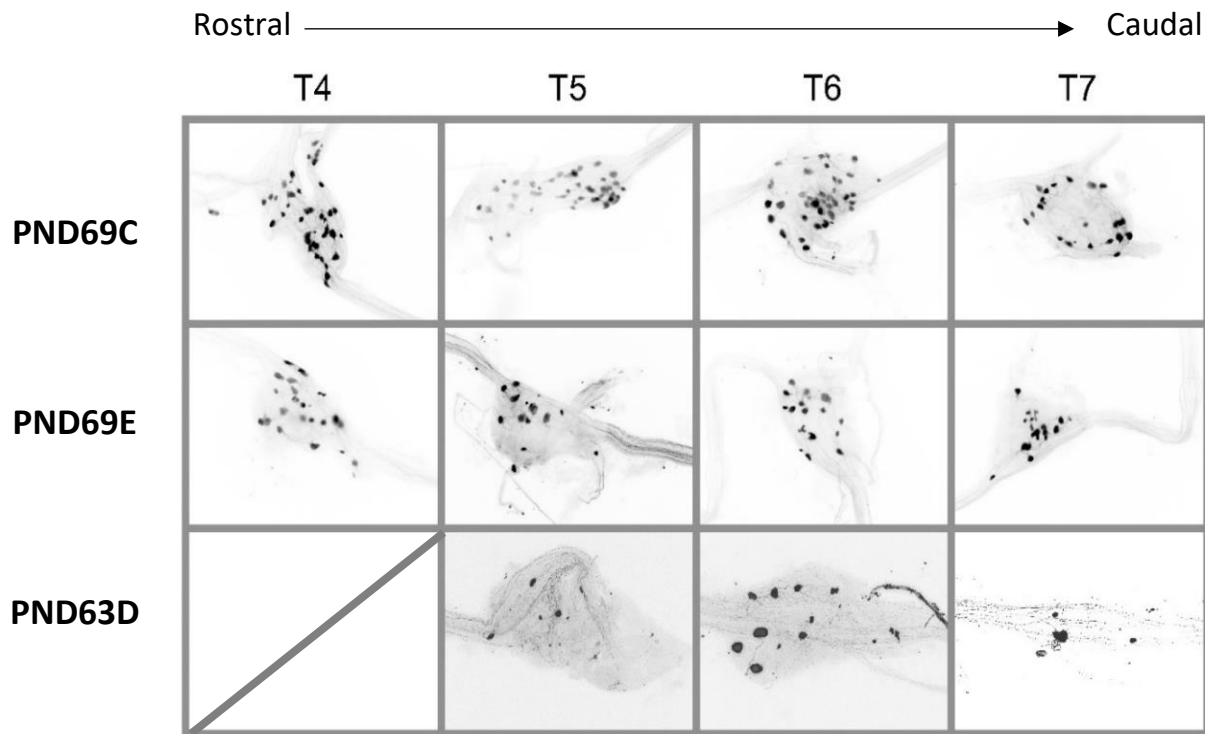


Figure 19: 4 consecutive thoracic ganglia of 3 adult mice

Starting with T4 and ending with the most caudal, T7. In these figures, neurons in dark black are the tdTomato+ cells. These were the cells counted for our initial rostro-caudal evaluation.

3.6 TH+ and Td+ Cell counts

To provide a provisional understanding of the relationship between Td+ number and the number of all cells in the ganglion I compared Td+ cell number to the total number of Th+ cells in two mice. TH+ cells were counted using Neurolucida (Olympus BX51 microscope, Optronics Microfire camera, 40x). Td+ neurons represented 6.15% and 5.66% of the total Th+ population suggesting a similar proportional expression of Td+ neurons in these animals. A Chi-Square test on Td+ populations as a percentage of the whole shows that these two adults are not significantly different at a 95% CI ($p=0.88$). The consistency in counts supports the theory that individual differences overpower rostrocaudal and developmental differences.

4. Conclusion

To summarize my results, I found the following morphological trends across development in Td+ post-ganglionic neurons in the fifth thoracic paravertebral sympathetic chain ganglia:

The *number of neurons* was **not** significantly different across age groups. The mean number of cell bodies shows PND 21 > PND 35 > PND 60+ in accordance with Masliukov (2001) who found that the number of neurons in the stellate ganglion in cats was highest in newborns and decreased up until 20 days post-natally. Nonetheless, a one-way ANOVA indicates no statistically significant difference between age groups. Possibly, a larger n is needed to reach any significant results.

The means of *cell body volume* did **not** vary significantly between age groups. Within age groups, the difference in the median values of cell body volume for the 3 PND 21 and 4 PND 60+ ganglia are statistically significant. If small is operationally defined as smaller than $1200\mu\text{m}^3$ and large as larger than $1200\mu\text{m}^3$ then 45.1%, 42.9% and 28.3% of PND 21, PND 35 and PND 60+ cell bodies are 'small'. Masliukov reported this same trend except their operational definition of small was neurons with a cell body CSA smaller than $200\mu\text{m}^2$. Furthermore, cell bodies larger than $4800\mu\text{m}^3$ were only seen in PND 35 and PND 60+ mice. In adolescence I observed the largest range of soma volume size, with both the smallest and largest cell body volumes noted. Albeit, numerically, large neurons ($>1200\mu\text{m}^3$) in PND 60+ (71.7%) make up a greater part of the population than do large neurons in PND 35 (57.1%).

CSA in non-reconstructed neurons **is** significantly different across development. CSA increased across the three age groups; that is, PND 21 > PND 35 > PND 60+. *Maximum perimeter* measures were **not** significantly different across age groups.

The *number of primary dendrites* **is** significantly different across developmental timepoints. Specifically, there are significantly more dendrites per neuron in PND 21 ganglia compared to PND 35. Therefore, there are more dendrites per neuron in younger mice as opposed to adolescent or adult mice. Individual variability across ganglia is seen in PND35 and PND 60+ but not in PND 21.

The *length of primary dendrites* **is** significantly different across developmental timepoints. When primary dendrite length was analysed by separating branched and un-branched primary dendrites, I found that mean values increased with age in both these dendrite categories. Following a pairwise comparison, branching dendrite length is significantly shorter in PND21 mice and length of un-branched dendrites was significantly greater in PND 60+ mice. No individual difference in length of primary un-branched dendrites was found, but an individual difference was seen in PND 21 mice in branched dendrite length between ganglia.

As for *branching* of primary dendrites, there **is** a significant difference across age groups. 48.7%, 68.7% and 25.7% of primary dendrites branched in PND 21, PND 35 and PND 60+ ganglia respectively. Thus, PND 60+ dendrites have the least amount of branching, followed by PND 21 and PND 35 in that order. Significant individual variation in branching was only seen when comparing PND 21 ganglia.

A rostro-caudal analysis of T4-T7 showed high variation amongst individuals that masked possible rostro-caudal differences in the chain. TH+ and Td+ neuron counts in 2 adults showed similar ratios of Td:TH cells in T5 with ~6% Td+ neurons.

5. Discussion

5.1 Implications of Morphological Trends: Dendritic Arborization

Morphological measures as discussed previously can provide significant insight on the functional properties of a neuron. Starting my discussion with dendritic complexity, I found conflicting results. Although primary dendrite length significantly increased across development, branching of primary dendrites and number of dendrites per neuron did not. In fact, there was a significant decrease in branching of primary dendrites during ontogenesis and PND 21 mice had the largest number of dendrites per neuron, as shown by a one-way ANOVA. This suggests that older mice have more complex dendritic arbors only when considering length. Although I did not fully reconstruct these dendrites and thus cannot report total dendritic length, it is interesting to note that the trend of increased dendritic length found in previous studies can be seen in primary dendrite length as well. More specifically, branching dendrite length is significantly shorter in PND21 mice and length of un-branched dendrites is significantly greater in PND 60+ mice. This suggests that it is not simply increased arborization and branching that leads to increased dendritic length but also growth of the primary process itself.

Branching of dendrites has been reported to increase across development (Snider, 1988, Voyvodic, 1987) but here I found the opposite. Of note, my analysis of branching differed from

Snider's and Voyvodic's as I only analyzed branching of primary dendrites and also had no measure of extent of branching. Thus assuming similar dendrite growth pattern across paravertebral ganglia, reconstruction of primary dendrites only is not sufficient to extrapolate total dendritic branching patterns. My analysis separating branched primary dendrites from unbranched primary dendrites showed that mean values increased across development and the difference amongst PND 21 vs. PND60+ was significant, allowing us to more confidently say that dendritic arborization increases across development. However, more research needs to be done in the mouse that includes measures of branching distal to that of primary dendrites to confidently evaluate differences from previous findings in other mammals.

Individual variation relating to dendritic complexity was highest in PND 21 mice. That is, for branching prevalence and primary branched dendrite length, individual variation between the PND 21 ganglia studied was significant at a 95% CI. However, PND 21 mice were the only group showing no significant individual difference in the number of dendrites per neuron between ganglia. This could suggest that PND 21 mice may represent a stage during development where primary dendrites are actively growing but that an event following PND 21 triggers branching and dendrite length homogeneity through dendritic pruning. Increased dendritic length across development suggests that after possible pruning, remaining dendrites grow to greater lengths.

, Previous research done on rats and guinea pigs is inconclusive in defining a trend in number of primary dendrites/neuron developmentally. An increase is reported in primary dendrite number from 6 weeks to 7 months in rat superior cervical ganglia (Andrews, 1993) and

early fetal to adult stages in the celiac ganglia of guinea pigs (Anderson et al., 2001). Voyvodic (1987a) reported that the number of primary dendrites increases in the first month of life and stabilizes beyond the first post-natal month. However, Snider reported no change in number of primary dendrites during post-natal development in the superior cervical ganglion of 1 week, 2 week and 8-week-old rats. Instead, he theorized that post-natal dendritic changes manifest themselves through increases in total dendritic length, extent of arbor and branching but not number (Snider, 1988). These hypothesis are conflicting and surprising considering most were conducted in the superior cervical ganglion of rats. This clearly shows why more research needs to be done to better understand the sympathetic nervous system as it seems to be incredibly variable even in the same ganglion of the same species.

Although no increase was seen, Snider (ref date) did not report a decrease in number of primary dendrites during development whereas I did, particularly during post--natal days 21 – 35. Voyvodic (1987) suggested that creation of primary dendrites is restricted to pre-natal or neo-natal time points in the rat. This seems to be a possibility in the mouse as well but my youngest time point was 3 weeks post-natally and thus I cannot determine whether the large number of dendrites in PND 21 is due to post-natal or prenatal growth. Research analyzing dendritic arborization of thoracic SPNs in neonatal mice is warranted in light of my findings.

Concerning dendritic complexity, an increased number of dendrites per neuron is not necessarily indicative of increased functional complexity, connectivity or communication as dendritic pruning shows that the animal is undergoing or has undergone refinement of neural networks (Schuldiner and Yaron, 2014).

5.2 Implications of Morphological Trends: Cell size

I used cell body volume as a measure of soma size, as opposed to previous work that used CSA or max perimeter, because new tools and technologies allow for the accurate reconstruction of soma volume, a more comprehensive measure of size. Interestingly, among the neurons for which I traced CSA CSA between groups was significantly different but perimeter was not suggesting issues with using either one of these parameters as measures of cell size.

Soma size has been seen to increase during post-natal development in mammals (Masliukov, 2002; Anderson et al., 1993) and is a measure that is functionally relevant as it correlates with number of primary dendrites and electrophysiological properties of neurons such as conduction velocity (Gibbins et al., 2000). In this study, the statistics on cell body volume data were very underpowered ($\alpha = 0.172$, desired $\alpha = 0.800$) and the individual variation in cell body volume was significant within PND 21 and PND 60+ ganglia.

On the significance of the trend seen in CSA across development, it is possible that CSA but not cell body volume was significantly different across development because only clustered neurons were contoured for CSA analysis. Contours of neurons instead of cell body volume reconstructions were necessary in 2 PND21 ganglia, 1 PND 35 ganglion and 1 PND 60+ ganglion. Possibly, if clustered neurons arose from the same lineage through post-natal neurogenesis, then these neurons would be morphologically more similar to each other than other neurons in the same ganglia. This and the fact that cell body volume included results from most neurons in all ganglia whereas CSA was only collected for a limited number of ganglia at each age group might have resulted in a decreased variability in CSA data allowing for statistical significance.

Furthermore, previous morphological studies used sharp microelectrode methods to fill neurons for morphological reconstruction. However, compared to other methods, this would bias labelling to those cells large enough to support tracer injection. It has been seen that different electrophysiological properties of thoracic SPNs are detected depending on if sharp electrode recording or whole-cell patch recording is used (McKinnon, 2019). This could explain why previous studies showed a significant change across development; they were sampling from the largest neurons in each ganglion, a possible functional subtype. In comparison the genetic method employed here would not bias towards a morphological subtype and would include sampling of neurons with very small to very large cell bodies.

Thus the genetic methods employed here may provide a more comprehensive assessment of the range of morphological properties of thoracic SPNs.

5.3 Individual and Rostro-caudal Variability

Previous work done in the lab suggests gross anatomical variability in the tSCG of mice (see *Figure 20*), therefore part of the goal of this study was to better understand the variability of the sympathetic nervous system amongst not only different age groups but also individuals.

This variability previously reported by McKinnon (2019) was seen in littermates, mice who share the same paternal and maternal genome, suggesting possible epigenetic contribution to SPN morphology. Morphological measures beyond gross anatomy were highly variable amongst naïve individuals and regardless of age. This was particularly relevant for cell body volume and number of neurons in a ganglion. Furthermore, although rostrocaudal variation amongst the ganglia has

been well documented, my rostrocaudal analysis showed that individual differences masked any rostral vs. caudal differences. A theory is that early life experience could play a significant role in the establishment of neural networks related to the sympathetic nervous system.



Figure 20: Tracings of the tSCG in adult mice

Littermates are boxed. Clearly detectable is the large anatomical differences amongst them, particularly in caudal rather than rostral ganglia. Caudal ganglia have more nerve outputs and are less uniform both in size and in placement across the different mice in these tracings. Diagram provided by Michael McKinnon, PhD at Emory University School of Medicine, Department of physiology.

Early life exposures can have profound effects on animal physiology by reprogramming developmental trajectories (Bolton and Bilbo, 2014). The extent to which developmental reprogramming occurs in tSCGs to impact autonomic function in the adult is not known. Studies on adult neurotransmitter availability in the superior cervical ganglion suggests that perinatal resource availability can influence SPN organization (Gaetani et al, 1975). My project

demonstrates that developmental changes in tSCG morphology occur after weaning and into adulthood. This developmental plasticity raises the possibility that tSCGs may be particularly susceptible to physiological and environmental stress in post-natal life and may contribute to developmental reprogramming of autonomic function.

5.5 *The Sparse Label*

Our TH+/Td+ cell counts revealed that the number of Td+ neurons as a percentage of the entire TH+ population was similar in the T5 ganglia of 2 different individuals. This gives us increasing confidence that Td+ expression is equally sparse in the ganglia analysed. Nonetheless, our n was very small, thus the significance of these findings is limited and with this uncertainty it is not possible to extrapolate findings in the Td+ population to all cells in a ganglion. Furthermore, comparison of neuron counts between animals based solely on number of Td+ labeled neurons is very underpowered and unreliable; thus moving forward, to assess age-dependent differences in neuron number, total neuron counts are needed.

Additionally, we cannot know for certain whether the sparse label is entirely random. In other words, did our sparse label select for a functional subtype of neuron for expression? For example, clusters of red fluorescent tdTomato neurons prevented reconstruction of some cell bodies in many ganglia (See *Figure 21*). A theory is that these clusters represent a clonal lineage arising from a single cell.

Although it is generally understood that adult neurogenesis is rare, cell proliferation in the nervous system outside that of the neocortex is poorly understood (Gonsalvez et al., 2013). In the central nervous system neuronal differentiation stimulates withdrawal from the cell cycle;

however, various studies have shown that this is not always the case in neurons of the sympathetic ganglia. It was noted that with age an increasing number of catecholamine producing neurons (including noradrenergic neurons) withdrew from the cell cycle, but a handful continued to divide (Rothman et al., 1978).

If expression of Td+ is not equal in all subpopulations a minor difference in initial expression of Td+ could be amplified during development thus biasing the particular tSCG phenotype. By the Grubb's test, the cell counts in the 4 different ganglia of PND 60+ mice showed a significant outlier (PND 69C, $p=0.037$). This may show individual variation or support for Td+ bias in a particular population due to division within a clonal lineage. Among the adult sample both Td+ number and Td+ clustering was greatest in PND 69C.

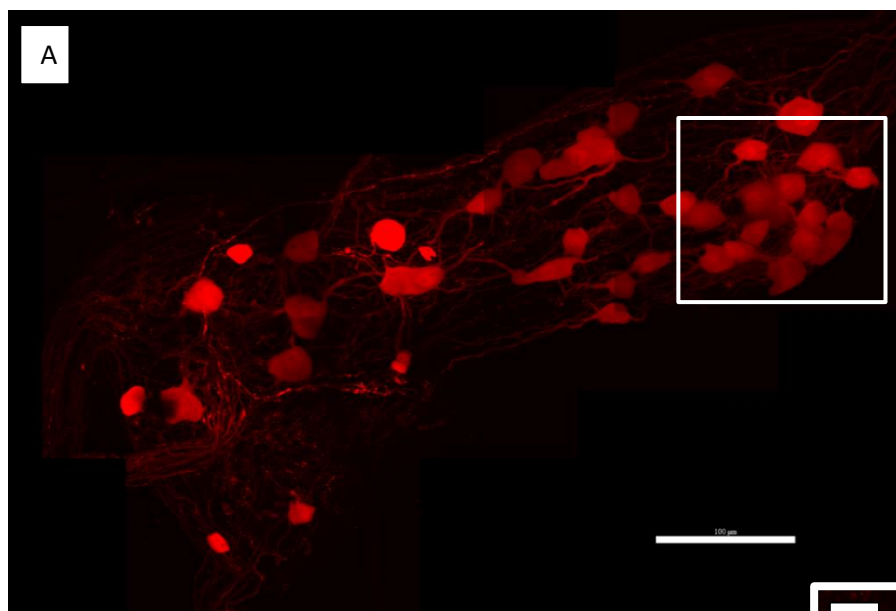
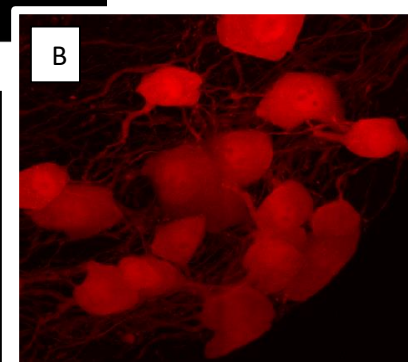


Figure 21: (A-E) T5 ganglia of PND69C.

A. Full T5 confocal image in PND69C

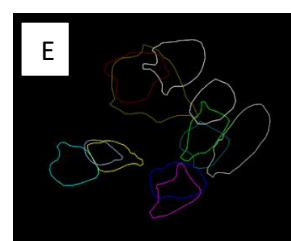
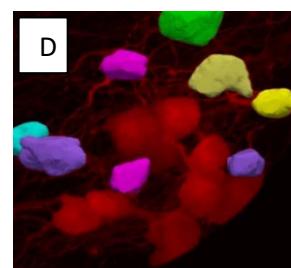
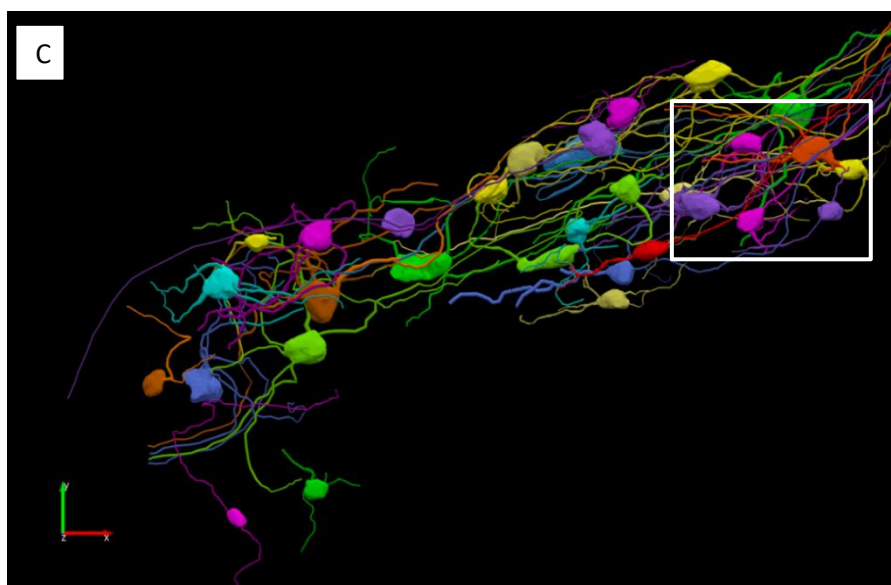
B. Zoomed in capture of a cluster of Td+ neurons found in this ganglion. This was not an isolated event as clusters were spotted in other animals of different ages. Namely in PND35A, PND21B and PND21C.



C.: This image shows the reconstruction of the T5 ganglia above of PND69C. Because of the proximity of Td+ neurons in the cluster, they could not be accurately reconstructed by the user-guided program.

D. Neurons that could not be reconstructed in the cluster shown in red. Instead they were contoured at what I visually determined was the maximal cross-sectional area across the Z stack.

E. Contours



5.6 Body Size as a Confounding Variable

Previous research indicates a strong relationship between dendritic complexity and body weight during development in the rat superior cervical ganglion (Voyvodic, 1987b). Purves and Lichtman in 1985 studied morphological differences in the superior cervical ganglion across different mammals of different sizes. They found that dendritic complexity varied according to body size with greater complexity in larger mammals. Additionally, neurons of progressively larger mammals were innervated by progressively more axons. Hence, body size may influence both morphological and functional features of sympathetic ganglion neurons. In my study, body weight was not recorded, but across development body weight increases and thus this could clearly be a confounding variable. In other words, the trends spotted could be not due to age but rather to changing body weight or possibly a combination of both.

6. References

Alshak M, Das J (2020) Neuroanatomy, Sympathetic Nervous System. Ncbi.nlm.nih.gov Available

at: <https://www.ncbi.nlm.nih.gov/books/NBK542195/> [Accessed March 24, 2020].

Anderson, R., Jobling, P. and Gibbins, I. (2001). Development of Electrophysiological and Morphological Diversity in Autonomic Neurons. *Journal of Neurophysiology*, 86(3), pp.1237-1251.

Andrews, T., Li, D., Halliwell, J., Cohen, T. (1993). The effect of age on dendrites in the rat superior cervical ganglion. *J. Anat.*, 184, pp.111-117.

Badea T, Hua Z, Smallwood P, Williams J, Rotolo T, Ye X, Nathans J (2009) New Mouse Lines for the Analysis of Neuronal Morphology Using CreER(T)/loxP-Directed Sparse Labeling. *PLoS*

ONE 4:e7859.

- Bolton J, Bilbo S (2014) Developmental programming of brain and behavior by perinatal diet: focus on inflammatory mechanisms. *Dialogues Clin Neurosci*:302-320.
- Bratton B, Davies P, Jänig W, McAllen R (2010) Ganglionic transmission in a vasomotor pathway studied in vivo: vasomotor ganglionic transmission in vivo . *J Physiol* 588:1647–1659. doi:10.1113/jphysiol.2009.185025
- Chelmicka-Schorr, E., Yu, R. C., Sportiello, M. G., & Arnason, B. G. (1985). Sympathetic ganglia augment growth of neuroblastoma in vitro. *European Journal of Cancer and Clinical Oncology*, 21(8), 957–964. doi: 10.1016/0277-5379(85)90115-4
- Choi M (2015) Anatomical survey of paravertebral sympathetic chain in adult mice.
- Curley, J. P., Jordan, E. R., Swaney, W. T., Izraelit, A., Kammel, S., & Champagne, F. A. (2009). The Meaning of Weaning: Influence of the Weaning Period on Behavioral Development in Mice. *Developmental Neuroscience*, 31(4), 318–331. doi: 10.1159/000216543
- Deuchars S, Lall V (2015) Sympathetic Preganglionic Neurons: Properties and Inputs. *Comprehensive Physiology*.
- Ernsberger U (2001) The development of post-ganglionic sympathetic neurons: coordinating neuronal differentiation and diversification. *Autonomic Neuroscience* 94:1-13.
- Furlan A, La Manno G, Lübke M, Häring M, Abdo H, Hochgerner H, Kupari J, Usoskin D, Airaksinen M, Oliver G, Linnarsson S, Ernfors P (2016) Visceral motor neuron diversity delineates a cellular basis for nipple- and pilo-erection muscle control. *Nature Neuroscience* 19:1331-1340.
- Gaetani S, Mengheri E, Spadoni M, Rossi A, Toschi G (1975) Effects of litter size on protein, choline

- acetyltransferase (CAT), and dopamine- β -hydroxylase (DBH) of a mouse sympathetic ganglion. *Brain Research* 86:75-84.
- Gibbins, I., Jobling, P., Messenger, J., Teo, E., & Morris, J. (2000). Neuronal morphology and the synaptic organisation of sympathetic ganglia. *Journal Of The Autonomic Nervous System*, 81(1-3), 104-109. doi: 10.1016/s0165-1838(00)00132-6
- Gonsalvez D, Cane K, Landman K, Enomoto H, Young H, Anderson C (2013) Proliferation and Cell Cycle Dynamics in the Developing Stellate Ganglion. *Journal of Neuroscience* 33:5969-5979.
- Havton L, Ohara P (1994) Cell body and dendritic tree size of intracellularly labeled thalamocortical projection neurons in the ventrobasal complex of cat. *Brain Research* 651:76-84.
- Hochman S (2015) Metabolic recruitment of spinal locomotion: intracellular neuromodulation by trace amines and their receptors. *Neural Regeneration Research* 10:1940.
- Huttenlocher PR. Synaptic density in human frontal cortex—developmental changes and effects of aging. *Brain Research*. 1979;163:195–205.
- Jänig W (2014) Sympathetic nervous system and inflammation: A conceptual view. *Autonomic Neuroscience* 182:4-14.
- Jänig, W. (2006). *The integrative action of the autonomic nervous system: Neurobiology of Homeostasis*, Cambridge, UK: Cambridge University Press.
- Jobling P, Gibbins I (1999) Electrophysiological and Morphological Diversity of Mouse Sympathetic Neurons. *Journal of Neurophysiology* 82:2747-2764.
- Kelmenson P (2020) Cre Lox Breeding for Beginners, Part 1. The Jackson Laboratory Available at:

<https://www.jax.org/news-and-insights/jax-blog/2011/september/cre-lox-breeding>

[Accessed March 28, 2020].

- Kenney, M. J., & Ganta, C. K. (2014). Autonomic Nervous System and Immune System Interactions. *Comprehensive Physiology*, 1177–1200. doi: 10.1002/cphy.c130051
- Lambert MS. Breeding Strategies for Maintaining Colonies of Laboratory Mice. TJ Laboratory; Bar Harbor: 2009. Breeding strategies for maintaining colonies of laboratory mice.
- Lichtman J, Purves D, Yip J (1980) Innervation of sympathetic neurones in the guinea-pig thoracic chain. *The Journal of Physiology* 298:285-299.
- Laviola G, Macri S, Morley-Fletcher S, Adriani W. Risk-taking behavior in adolescent mice: psychobiological determinants and early epigenetic influence. *Neuroscience & Biobehavioral Reviews*. 2003;27:19–31
- Masliukov, P. (2001). Sympathetic neurons of the cat stellate ganglion in postnatal ontogenesis: morphometric analysis. *Autonomic Neuroscience*, 89(1-2), pp.48-53.
- Masliukov P, Timmermans J (2004) Immunocytochemical properties of stellate ganglion neurons during early postnatal development. *Histochemistry and Cell Biology* 122:201-209.
- McKinnon M, Tian K, Li Y, Sokoloff A, Galvin M, Choi M, Prinz A, Hochman S (2019) Dramatically Amplified Thoracic Sympathetic Postganglionic Excitability and Integrative Capacity Revealed with Whole-Cell Patch-Clamp Recordings. *eneuro* 6:ENEURO.0433-18.2019.
- Nunez-Abades Pa and Cameron. Morphology of developing rat genioglossal motoneurons studied in vitro: relative changes in perimeter and surface area of somata and dendrites. *J Comp Neurol* 353: 129–142, 1995.

Purves, D., & Lichtman, J. (1985). Geometrical differences among homologous neurons in mammals. *Science*, 228(4697), 298-302. doi: 10.1126/science.3983631

Purves D, Hadley R, Voyvodic J (1986) Dynamic changes in the dendritic geometry of individual neurons visualized over periods of up to three months in the superior cervical ganglion of living mice. *The Journal of Neuroscience* 6:1051-1060.

Reid I (1992) Interactions between ANG II, sympathetic nervous system, and baroreceptor reflexes in regulation of blood pressure. *American Journal of Physiology-Endocrinology and Metabolism* 262:E763-E778.

Rohrer H, Thoenen H (1987) Relationship between differentiation and terminal mitosis: chick sensory and ciliary neurons differentiate after terminal mitosis of precursor cells, whereas sympathetic neurons continue to divide after differentiation. *J Neurosci* 7:3739–3748

Romijn HJ, Hofman MA, Gramsbergen A. At what age is the developing cerebral cortex of the rat comparable to that of the full-term newborn human baby? *Early Human Development*. 1991;26:61–67

Rothman TP, Gershon MD, Holtzer H (1978) The relationship of cell division to the acquisition of adrenergic characteristics by developing sympathetic ganglion cell precursors. *Dev Biol* 65:322–341

Savitt J (2005) Bcl-x Is Required for Proper Development of the Mouse Substantia Nigra. *Journal of Neuroscience* 25:6721-6728.

Schafer M, Schutz B, Weihe E, Eiden L (1997) Target-independent cholinergic differentiation in the rat sympathetic nervous system. *Proceedings of the National Academy of Sciences* 94:4149-4154.

Schuldiner O, Yaron A (2014) Mechanisms of developmental neurite pruning. *Cellular and Molecular Life Sciences* 72:101-119.

Snider W (1986) Rostrocaudal differences in dendritic growth and synaptogenesis in rat sympathetic chain ganglia. *The Journal of Comparative Neurology* 244:245-253.

Snider W (1988) Nerve growth factor enhances dendritic arborization of sympathetic ganglion cells in developing mammals. *The Journal of Neuroscience* 8:2628-2634.

Springer MG, Kullmann PHM, Horn JP (2015) Virtual leak channels modulate firing dynamics and synaptic integration in rat sympathetic neurons: implications for ganglionic transmission in vivo. *J Physiol* 593:803–823. doi:10.1113/jphysiol.2014.284125

Szurszewski, Joseph H. and Linden, David R. , in *Physiology of the Gastrointestinal Tract* (Fifth Edition), 2012

Voyvodic J (1987a) Development and regulation of dendrites in the rat superior cervical ganglion. *The Journal of Neuroscience* 7:904-912.

Voyvodic, J. (1987b) Development and regulation of dendrites in the rat superior cervical ganglion: Influence of preganglionic innervation. *J. Neurosci.* 7: 904-912.

Watkins K (2018) The effect of spinal cord injury on C-fiber low-threshold mechanoreceptors and sensory afferents that transiently express tyrosine hydroxylase.

Zshabotinsky, J.M., 1953. *Normal and Pathologic Morphology of the Autonomic Ganglia*. AMS USSR, Moscow, 292 pp. in Russian.